Title
The Role of Gap Junction Communication in Lens Transparency: A Potential Strategy for Cataract Prevention

Author
Li, Lin

Publication Date
2009

Peer reviewed|Thesis/dissertation

The Role of Gap Junction Communication in Lens Transparency: A Potential Strategy for Cataract Prevention

by

Lin Li

A dissertation submitted in partial satisfaction of the

requirements for the degree of

Doctor of Philosophy

in

Vision Science

in the

Graduate Division

of the

University of California, Berkeley

Committee in charge:

Xiaohua Gong, Chair
Suzanne M.J. Fleiszig
Song Li

Fall 2009

The dissertation of Lin Li is approved:

Chair _____ Date _____

_____ Date _____

_____ Date _____

University of California, Berkeley

Fall 2009

The Role of Gap Junction Communication in the Lens: Potential Strategies for Cataract Prevention

by Lin Li

Abstract

The Role of Gap Junction Communication in Lens Transparency:
A Potential Strategy for Cataract Prevention

by

Lin Li

Doctor of Philosophy in Vision Science

University of California, Berkeley

Professor Xiaohua Gong, Chair

Approved:

Chair _____ Date _____

Abstract

The ocular lens must maintain transparency and a high refractive index throughout life in order to transmit a clear light image onto the retina. Cataracts, defined as any lens opacity, are one of the major causes for vision impairment in the world. A non-surgical way to either prevent or delay cataract formation will significantly improve vision care and reduce eye Medicare cost. By studying cataractogenesis at the genetic, morphological, histological and biochemical levels, my thesis project has provided some new understanding of the molecular mechanisms that maintain lens homeostasis, and has demonstrated the suppression of a congenital cataract through a genetic method.

My thesis includes three parts: 1) To study the molecular basis for the nuclear cataract formation in γB-S11R mutant mice; 2) To study how does elevation of α3 connexin in the lens, expressed from the knock-in (Ki) α3 gene, prevent the nuclear cataract caused by the γB-S11R mutation; 3) To identify a genetic modifier of the C57BL/6J mouse strain background that dominantly suppresses the nuclear cataract caused by the α3 null mutation.

We have determined that a dominant nuclear cataract, linked to the γB-crystallin S11R point mutation, was associated with abnormal γ-crystallin protein aggregation and disrupted membrane-cytoskeleton structures of inner lens fiber cells (Li et al., 2008). Moreover, increases of lens calcium level and calcium-dependent protein degradation were related to the degeneration of inner mature fiber cells and the nuclear cataract formation of γB-crystallin S11R mutant lenses, similar to that ofα3 connexin (Gja3 or Cx46) homozygous knockout lenses. Thus, similar mechanisms probably associated with nuclear cataract formation in both γB-S11R crystallin and α3 connexin mutant lenses.

Knockin α3 (Ki α3) connexin under endogenous α8 connexin (Gja8 or Cx50) gene promoter is known to improve gap junction formation to suppress cataracts caused by α8-G22R connexin mutation (Xia et al., 2006b). In order to evaluate whether improved gap junction communication mediated by Ki α3 could suppress the nuclear cataract caused by γB-S11R mutation, we have generated Ki α3 and γB-S11R compound homozygous mutant mice. Unlike the dense nuclear cataracts in γB-S11R mutant mice, these compound mutant micedisplayed clear lenses with relatively well-organized fiber cells. Immunohistochemistry data revealed normal distribution of actin filaments and cytosolic γ-crystallins. Compound mutant lenses had no obvious increase of crystallin protein degradation and total lens calcium level remained similar to that of wild-type lenses. Thus, elevation of gap junction communication via knockin α3 connexin prevents lens calcium elevation which probably inhibits calcium-dependent protein degradation and prevents fiber cell degeneration.

It is known that other genetic factor(s) influences the severity of nuclear cataracts in α3 connexin knockout mice between 129/SvJ or C57BL/6J strain backgrounds (Gong et al., 1999; Gong et al., 1997). In order to identify the genetic suppressor in C57BL/6J α3 knockout mice, we generated α3 knockout mice at the C57BL/6J x 129/SvJ hybrid strain backgrounds. Genome-

wide genetic linkage testing and fine mapping located a genetic modifier in a region about two centimorgans on chromosome 7. This genetic modifier of C57BL/6J strain background can suppress dense nuclear opacity resulted from a loss of α3connexin in the lens.. The severity of nuclear cataracts was correlated to the amount of cleaved forms of crystallin proteins in α3 knockout lenses. This genetic suppressor may regulate calcium homeostasis to inhibit the activities of calpain proteases in the lens. by

This thesis demonstrates for the first time that upregulation of gap junction communication can prevent a nuclear cataract caused by a γB-crystallin gene mutation. Moreover, a genetic suppressor functions on the upstream of calpain proteases to suppress a nuclear cataract caused by gap junction communication composed by α3 connexin in the lens. Understanding the roles of gap junction communication and related genetic modifier(s) are important for developing a potential strategy for nuclear cataract prevention in the future.

for Isabelle and Shanshan
&
Dedication to Gong Lab

Acknowledgements

This dissertation is dedicated to the love of my dear mother, Shanshan Huang. Being a single mother for 25 years, she has taken care of me in all situations to the best of her ability. I have received excellent education, sufficient financial support, positive influence, and binding love. She is a Buddhist who lived her life well, acting upon her spiritual beliefs conscientiously by assisting both friends and strangers in need. She faced difficulties bravely. I understand how hard it was being a single mother and coming to the United States without knowing English. Her spirit kept me working when I wanted to give up. This dissertation is also dedicated to my dear wife, Isabelle Sun. We fell in love and married each other during my graduate school career. She has been extremely supportive. Please believe me, Isabelle, I love you much more than I love science because I spend more time with you.

My appreciations also go to Dr. Xiaohua Gong, my thesis advisor, for his mentorship and encouragement for me to complete the research project and my dissertation throughout these years. The inspiration for my pursuit of a Ph.D. in Vision Science came from him. He spotted me out of hundreds of Bioengineering applicants when he served as a member of admission committee at The UCSF-UCB Joint Graduate Studies in Bioengineering, transferred me to the Vision Science program, and accepted me as a graduate student in his lab. My career in the Vision Science program was one of the most important and formative experiences in my life. Dr. Gong has consistently helped me keep perspective on what is important in life and has shown me how to deal with reality. I am grateful as well to Frances B. Stone and Inez S. Bailey for coordinating and overseeing the administrative concerns, making it possible for me to complete my degree.

The members of my dissertation committee, Dr. Xiaohua Gong, Dr. Suzanne M.J. Fleiszig and Dr. Song Li, as well as two other qualifying exam committee members, Dr. John G. Flannery and Dr. Clifton M. Schor, have generously given their time and expertise to better my work. I thank them for their contributions and their good-natured support.

I must acknowledge as well the many friends, colleagues, students, and teachers who have assisted, advised, and supported my research and writing efforts over the years. I especially need to express my gratitude and deep appreciation to the members of the Gong laboratory, including Dr. Chun-hong Xia, Dr. Catherine Cheng, Dr. Haiquan Liu, Dr. Kaijun Wang, Serena Tseng, Jennifer Lee, Peggy Lee, Stanley Ng, Lauri Shinn, Sheldon Leong and Desiree Cadiz for their help, friendship, knowledge and wisdom.

I am grateful to many other professors for their collaborative efforts and for sharing their expertise and lab facilities, especially the gel filtration and 2-D protein analysis of Dr. Joseph Horwitz's lab at UC Los Angeles, confocal microscopic analysis of Dr. Song Li's lab at UC Berkeley, genetic studies of Dr. Bo Chang at Jackson Laboratory and Dr. Thomas W. White at SUNY, Stony Brook.

My thanks must go also to my former mentors Dr. Weidong Xie at St. Jude Children's Hospital and Dr. Xuebiao Yao at University of Science and Technology of China. They led me into the fascinating life science research. Without them, I may have become a chemist.

I am very grateful for the support I received from the National Institute of Health during the two year training grant. My thanks also go to ARVO, ICER and the UC Berkeley graduate division for travel grant supports that allowed me to attend international eye conferences.

Table of Contents

List of Figures and Tables

Chapter 1 Basic Biology of the Lens and Cataract

1.1 Preface of Chapter

A cataract is a clouding of the lens in the eye that affects vision. Most cataracts are related to aging. Cataracts are very common in older people. By age 80, more than half of all Americans either have a cataract or have had cataract surgery. The medical cost in the U.S. for treating cataracts is over several billion dollars annually and there is no non-surgical method to treat cataracts. The lens is made of mostly water and proteins. Proteins are arranged in a precise way that keeps the lens clear and lets light pass through. At the cellular level, the lens is composed of a bulk of elongated fiber cells covered by a monolayer of epithelial cells on the anterior surface. Surface epithelial cells differentiate into elongated fiber cells at the lens equator, and newly differentiated fiber cells surround previous generations of fiber cells in a concentric manner. The gap junction channels formed by α3 and α8 connexins have been reported to couple the lens fiber cells during the formation of an avascular transparent lens. Small molecules such as calcium and other metabolites go through gap junctions in the lens. Genetic studies of α3 and α8 connexins reveal that they are crucial to maintain lens transparency. In the first chapter, I will introduce some basic terminologies, concepts and background information.

1.2 The Lens

The lens is a transparent, biconvex structure in the eye, between the cornea and retina. The lens, by changing shape through zonular fibers attached to the ciliary body, functions to change the focal distance of the eye. This allows for focusing at various distances in order to form a clear image of the object of interest on the retina. This adjustment of the lens is known as accommodation.

The lens is also known as a crystalline lens, and is comprised of three main parts: the lens capsule, the lens epithelium, and the lens fibers. The lens capsule forms the outermost layer of the lens and the lens fibers form the bulk of the interior of the lens. The lens epithelium, located between the lens capsule and the outermost layer of lens fibers, is only on the anterior side of the lens (Figure 1).

The lens capsule is the outer-most tissue that forms a basement membrane surrounding the lens. It is comprised of Type IV collagen and sulfated glycosaminoglycans (GAGs) that are synthesized by the lens epithelium (Forrester et al., 1996; John Forrester, 1996). Its elasticity and smoothness allow the lens to change and maintain its shape at different accommodation stages.

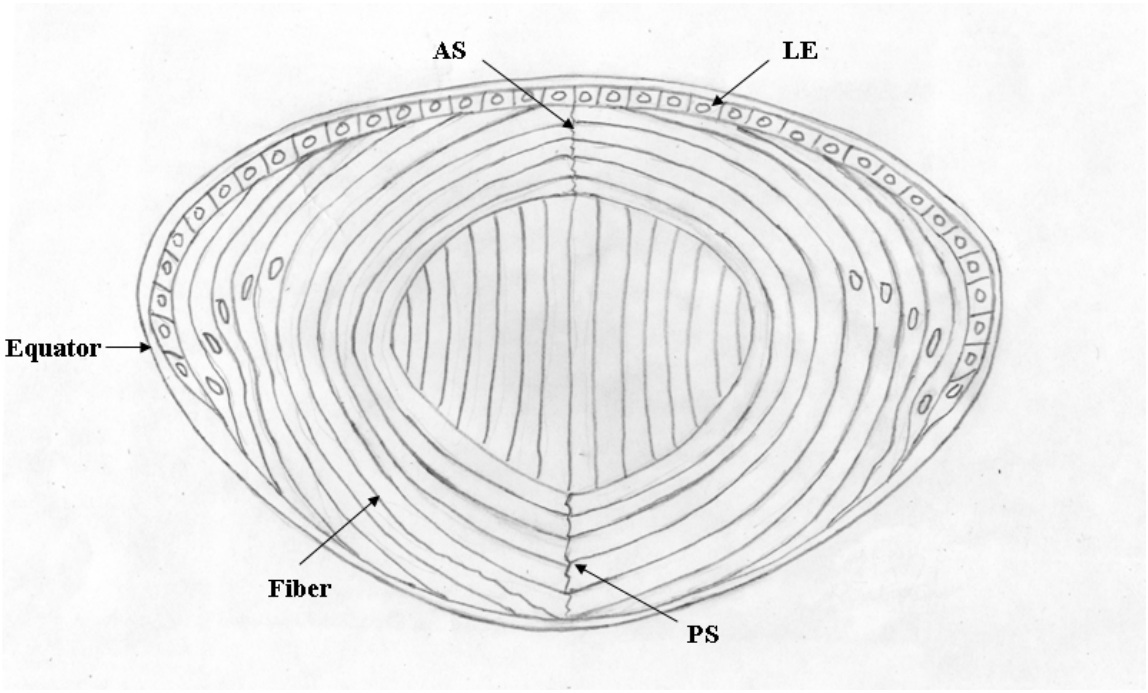

Figure 1. Cellular organization of the human lens. The lens consists of two cell types: lens epithelial cells (*LE*), which are a monolayer of epithelial cells at the anterior hemisphere of the lens, and concentric layers of fiber cells (*Fiber*) which occupy bulk of the interior of the lens. Fiber cells proliferate and differentiate continuously at the germinative zone near the lens equator (*Equator*). Newly-differentiated fiber cells are added at the periphery. The two ends of fibers extending from opposite hemispheres meet at the anterior (*AS*) and posterior (*PS*) sutures. During differentiation, fiber cells lose their cell organelles such as nuclei, ER, mitochondria and other organelles.

The lens epithelium is a monolayer of cuboidal shaped epithelial cells (Forrester et al., 1996). It regulates most of the homeostatic functions of the lens (Candia, 2004). Na+/K+ ATPase pumps in the lens epithelium pump ions, nutrients and water out of the lens to maintain appropriate lens osmolarity and volume. The lens epithelium also serves as the progenitors for embryonic and secondary lens fibers. In the embryonic stage, the lens epithelium at the posterior of the lens elongates to fill the middle of lens vesicle, forming the embryonic nucleus. The remaining lens epithelium constantly proliferates and differentiates at the germinative zone to become secondary fiber cells, and continues to lay down fibers at the periphery for lifelong growth (McAvoy et al., 1999; Piatigorsky, 1981).

The lens fibers are long, thin, transparent cells forming the bulk of the lens (Forrester et al., 1996). The lens fibers stretch lengthwise from the posterior to the anterior poles in a concentric manner, rather like the layers of an onion. However, the lens is not like an onion because new lens fibers are added on from the periphery, while onion cells expand from the core. The tips of the fibers extending from opposite hemispheres meet at the anterior and posterior sides to form Y-shape sutures. The lens fibers are linked together via gap junctions and interdigitations (also known as “ball and socket” structure of the fiber cells).

Another important factor that maintains lens transparency is the absence of light-scattering organelles such as the nucleus, endoplasmic reticulum, and mitochondria within the mature lens fibers (Bassnett, 2002). Lens fibers also have a very extensive cytoskeleton and beaded filament network that maintains the precise shape and packing of the lens fibers; disruptions of these elements can lead to cataract formation (Bloemendal et al., 2004).

Crystallins are water-soluble proteins that comprise over 90% of the protein within the lens (Hoehenwarter et al., 2006). The three main crystallin types found in the eye are α-, β-, and γ-crystallins. Lens transparency and high refractive index are believed to be maintained by the special arrangement and tight packing of crystallin proteins. Alpha-crystallin belongs to a small heat shock protein family and forms polydispersed heteromeric aggregates of αA-crystallin and αB-crystallin (Horwitz, 2000). Beta and γ-crystallins are mainly lens structural proteins that belong to β/γ-superfamily sharing a common Greek motif (Bloemendal et al., 2004). Beta-crystallins form oligomers while γ-crystallins appear as monomers. Beta and γ-crystallins are found primarily in the lens, while subunits of α-crystallin have been isolated from other parts of the eye and the body. α-crystallin proteins have chaperone-like activity *in vitro* which can prevent abnormal protein aggregation and help denature protein refolding (Horwitz, 1992). The chaperone functions of α-crystallin may also help maintain the health of lens proteins, which must last for a human’s entire lifetime (Andley, 2007).

Lens homeostasis is hypothesized to be maintained by gap junction communication (Mathias et al., 1997). Gap junction allows direct electrical and chemical communication between cells, although the channel conductance and selectivity are controlled by connexin subunits. Molecules smaller than 1,200 Daltons can pass through gap junctions, while large biomolecules, such as DNA and protein, are excluded. Mathias’ current circulation model

proposes that small molecules such as water and ions enter the cell by chemical gradients from the anterior and posterior, go through gap junctions to reach the peripheral epithelium and exit from the lens equator (Mathias et al., 1997).

There are at least three connexin subunits in the mammalian lens: α1 (Cx43), α3 (Cx46) and α8 (Cx50) (Goodenough, 1992; Musil and Goodenough, 1990; Paul et al., 1991; White et al., 1992). α1 connexin is only found in lens epithelium while α3 connexin is fiber cell specific (Beyer et al., 1989; Gong et al., 1997). α8 connexin is expressed in both lens epithelial cells and fiber cells (Dahm et al., 1999; Rong et al., 2002).

Aquaporin0 (AQP0) is an integral membrane protein that belongs to the aquaporin family of water transporters (Park and Saier, 1996). AQP0 is also known as major intrinsic protein (MIP) that is the most highly expressed membrane protein in the lens. AQP0 has water channel activity at physiological pH and low calcium concentration condition in the lens (Nemeth-Cahalan and Hall, 2000).

Lens fiber membrane intrinsic protein (Lim2, also known as Mp19 or Mp20) is the second most abundant lens membrane protein. The specific function of Lim2 is unknown. This protein appears to contain four transmembrane domains, is a substrate for cAMP-dependent protein kinase and protein kinase C, and binds with calmodulin. Taken together, these suggest that Lim2 functions in some way as a junctional component, possibly involved with lens cell communication. It has been shown to be involved with cataractogenesis (Shiels et al., 2007; Steele et al., 1997; Steele et al., 2000).

Actin filaments are the major cytoskeletal structure in the lens, however, beaded filaments are a type of intermediate filament unique to the lens fiber cells. Beaded filaments are made up of BFSP1 (also called CP115 or filensin) and BFSP2 (also called CP49 or phakinin). These proteins combine in the presence of α-crystallin to form the appropriate beaded structure. Beaded filaments are found in the differentiating fibers, but are not present in the epithelial cells. Beaded filaments initially locate near the plasma membrane, but become more cytoplasmic as fiber cells age (Blankenship et al., 2001; Sandilands et al., 1995).

1.3 Cataract

A cataract is defined as any clouding that develops in the crystalline lens of the eye or in its envelope (also called lens capsule), varying in degree from slight to complete opacity and obstructing the passage of light onto retina. Typically, as a cataract becomes more opaque, visual acuity and contrast sensitivity are compromised, so that contours, shadows and color vision are less vivid. Cataract patients normally see a veiling glare as light is scattered by the cataract in the lens. If untreated, cataracts progress slowly or rapidly to cause vision loss and potentially blindness (Quillen, 1999).

Cataract formation is associated with variety risk factors including long-term ultraviolet (UV) light exposure, radiation exposure, side effects of diseases such as diabetes, hypertension and advanced age, eye injury or physical trauma; they are usually a result of denaturation of lens protein. A recent study has shown that commercial airline pilots are three times more likely to develop cataracts than people with non-flying jobs (Rafnsson et al., 2005). Astronauts are at increased risk for developing cortical cataracts and higher space radiation doses may induce posterior subcapsular cataracts (Chylack et al., 2009). They are thought to be caused by excessive exposure to radiation coming from outer space. Cataracts are also unusually common in persons exposed to infrared radiation, and exposure to microwave radiation can cause cataracts (Kurz and Einaugler, 1968; Lydahl, 1984). Some drugs can induce cataract development, such as corticosteroids (Greiner and Chylack, 1979; Spencer and Andelman, 1965). However, congenital cataracts are often caused by genetic mutations in lens protein genes including lens crystallins, gap junction proteins, membrane proteins, beaded filament proteins, growth and transcriptional factors and some other proteins (Hejtmancik, 2008).

Age-related cataracts are responsible for 48% of the world's blindness, which represents about 18 million people, according to the World Health Organization (WHO). In many developing countries where surgical services are inadequate, cataracts remain the leading cause of blindness. However, cataracts are also an important cause of low vision in developed countries. As populations age, the number of people with cataracts is growing. In the Unites States, when baby boomers turn older, the need for cataract surgery will expand dramatically, bringing a huge burden to medical services and federal Medicare programs.

In the United States, age-related lenticular changes have been reported in 42% of those between the ages of 52 to 64 (Sperduto and Seigel, 1980), 60% of those between the ages 65 and 74 (Kahn et al., 1977), and 91% of those between the ages of 75 and 85 (Sperduto and Seigel, 1980). The following table 1 is a common classification of the various types of cataracts.

Classified by Etiology		
Age-related Cataract	**Congenital Cataract**	**Secondary Cataract**
Immature senile Cataract (IMSC)	Sutural Cataract	Drug-induced Cataract
Mature senile Cataract (MSC)	Lamellar Cataract	
Hypermature senile Cataract (HMSC)	Zonular Cataract	
	Total Cataract	
Classified by Location of Opacity within Lens Structure		
Anterior Cortical Cataract	Anterior Polar Cataract	Anterior Subcapsular Cataract
Posterior Polar Cataract	Posterior Subcapsular Cataract	After-cataract-posterior Capsular Opacification (PCO)
Nuclear Cataract	Posterior Cortical Cataract	

Table 1. Classification of the various types of cataracts

Cataract surgery is usually performed by an opthamologist to restore vision. When a cataract is sufficiently developed to be removed by surgery, the most effective and common treatment is to make an incision (capsulotomy) into the capsule of the cataractous lens in order to surgically remove the lens material. There are two types of eye surgeries that can be used to remove cataracts: extracapsular cataract extraction (ECCE) and intracapsular cataract extraction (ICCE).

Extracapsular cataract extraction consists of removing the lens but leaving the majority of the lens capsule intact while intracapsular cataract extraction involves removing the entire lens of the eye, including the lens capsule, but it is rarely performed in modern practice. In either ECCE or ICCE surgery, the cataractous lens is removed and replaced with an intraocular lens (IOL) which stays in the eye permanently. Complications are possible after cataract surgery, including inflammation, increase of intraocular pressure (IOP), posterior capsular opacification and retinal detachment.

Although cataracts have no scientifically proven prevention, it is sometimes said that wearing ultraviolet-protecting sunglasses may slow the development of cataracts (Neale et al., 2003). Regular intake of antioxidants (such as vitamin A, C and E) is theoretically helpful, but taking them as a supplement has been shown to have no benefit (Klein et al., 2006)1.4 Gap Junction in the Lens

A gap junction is an organized intercellular connection between cell membranes that allow small molecules to pass between adjacent cells, directly connecting their cytoplasm. Each gap junction channel consists of two connexons, one in each cell membrane. The two connexons of adjacent cells align, forming a continuous aqueous pathway by which ions and small molecules can freely and passively pass from one cell to the other. Each connexon consist of six subunits called connexins. In vertebrates, gap junction hemichannels are primarily homo- (two identical hemichannels) or hetero-hexamers (differing hemichannels) of connexin proteins. Several hundreds of gap junctions assemble into a macromolecular complex called a gap junction plaque.

Lens homeostasis is hypothesized to be maintained by gap junction communication (Mathias et al., 1997). Gap junction allows direct electrical and chemical communication between cells, although the channel conductance and selectivity are controlled by connexin subunits. Molecules smaller than 1,200 Daltons can pass through gap junctions, while large biomolecules, such as DNA and protein, are excluded. Mathias' current circulation model proposes that small molecules such as water and ions enter the cell by chemical gradients from the anterior and posterior, go through gap junctions to reach the peripheral epithelium and exit from the lens equator (Mathias et al., 1997).

Up to date, five different functions have been described to gap junction protein: 1) Electrical and metabolic coupling between cells; 2) Electrical and metabolic exchange through hemichannels; 3) Tumor suppressor genes (Cx43, Cx32 and Cx36); 4) Adhesive function independent of conductive gap junction channels; 5) Role of carboxyl-terminal in signaling cytoplasmic pathways (Cx43)

There are at least three connexin subunits in the mammalian lens: α1 (Cx43), α3 (Cx46) and α8 (Cx50) (Goodenough, 1992; Musil and Goodenough, 1990; Paul et al., 1991; White et al., 1992). α1 connexin is only found in lens epithelium while α3 connexin is fiber cell specific (Beyer et al., 1989; Gong et al., 1997). α8 connexin is expressed in both lens epithelial cells and fiber cells (Dahm et al., 1999; Rong et al., 2002).

1.4 Gamma-crystallins

The crystallins are the main structural proteins of the vertebrate eye lens. The β- and γ-crystallins share a common β sheets in the protein known as "Greek key motif", which occur four times in all members of the β- and γ-crystallin super family (Bloemendal et al., 2004). It is hypothesized that β/γ-crystallins evolved from ancestral genes coding for just one Greek key motif or two Greek key motifs (Antuch et al., 1996; Ohki et al., 2001; Shimeld et al., 2005). The function of the Greek key motif is still under debate, but there are three proposed functions: 1) Computation modeling suggests that Greek key motifs form an interdomain association in the β/γ-crystallins which allows a dense packaging of the proteins minimizing light scattering, but providing an optimum in high refractive index and transparency of the eye lens (Mills et al., 2007); 2) Greek key motif has been shown to have calcium binding properties (Sharma et al., 1989). γ-crystallins was identified as a calcium binding protein (Rajini et al., 2001). Other proteins with Greek key motifs also have calcium binding activity, such as protein S (Wenk et al., 1999) or spherulin 3a (Clout et al., 2001). This finding might have important implications for the understanding of cataractogenesis in which β/γ-crystallins are involved (Duncan and Wormstone, 1999; Sanderson et al., 2000); 3) This new function may not have to do with the Greek key motif, but recent study has shown β/γ-superfamily proteins are the lens-derived activators of cascades, which lead to axonal regeneration in culture retinal ganglion cells, and has suggested that their effects might be mediated by astrocyte-derived ciliary neurotrophic factor (CNTF) (Fischer et al., 2008).

In mouse, the γ-crystallin encoding genes (Cryg) are located at a cluster of five genes (Cryga to Cryge) within approximately length of 50 kb on chromosome 1. The sixth gene Crygf is present ~0.9 million base pair apart from this cluster and there are a few other genes located in between. All six Cryg genes are highly homologous, protein sequences of γE- and γF-crystallin are identical (Graw et al., 1991; Graw et al., 1993).

There are three exons in Cryg genes; the first exon is very short followed by a short intron. The second exon and the third exon encode two Greek key motifs respectively, separated by a large intron. The non-translated 3'-end is short. The Cryge and Crygf genes are pseudogenes in human, but they are strongly expressed in rodent embryonic and new-born stages (Brakenhoff et al., 1990).

The Cryg genes are expressed in mouse lenses from embryonic day 13.5 (E13.5) onwards in the primary fibers, and later on in the secondary fiber cells. However, expression is not found in the epithelial cells. The expression level reaches the maximum in mice at birth, and decreases during the first weeks after birth, however in human, the Cryg expression is restricted to prenatal development (Graw, 1997, 2009).

Gamma-Crystallins appear as monomeric structure in the lens. Monomer size is about 20 kDa so that gel-filtration chromatography of lens proteins shows γ-Crystallins in the last peak. They are the most basic crystallin proteins and contain a high content of Cysteine residues. Isoelectric points (PI) of γ-Crystallins range from 7.1 to 8.6. Sequence alignment data characterize the six γ-crystallins into two groups: γA/B/C-crystallins and γD/E/F-crystallins

(Graw, 1997). The temperature causing phase separation is different: low for the γA/B/C-crystallins and high for the γD/E/F-crystallins. Change of hydrophobicity and hydrophilicity in γD-crystallin compared to γB-crystallin might explain the property difference in phase separation (Norledge et al., 1997).

Various mutations in the Cryg genes causing cataract in mouse and human have been identified and characterized. From the first Cryg mutation Elo (Eye lens obsolesence) mutant mouse to some recent Cryg mutations found from our laboratory, more than 20 mutations in all of the six Cryg genes cluster at mouse chromosome 1 have been reported (Graw, 2009); all of them develop dominant congenital or age-related cataracts varying from mild opacities to severe cataracts with microphthalmia or lens rupture. Since the human CRYGE and CRYGF genes are pseudogenes, in contrast to the mouse, cataract-causing CRYG mutations in human patients have been only detected in the CRYGC and CRYGD genes (Graw, 2009). However, similar to the mouse situation, the lens phenotypes of human patient vary significantly.

In some Cryg mutant strains, the phenotypic alterations are first observed in embryonic stage (Oda et al., 1980; Santhiya et al., 1995); while some mutant mice develop age-related cataracts after the mice are born (Li et al., 2008; Liu et al., 2005). Sandilands' study presents evidence that the formation of intranuclear inclusions is a key event in cataractogenesis (Sandilands et al., 2002). In the *L23* mutant strain, congenital cataracts in the mouse involving Crygd-V76D mutations, large inclusions containing the γ-crystallins were found in the nuclei of the differentiating fiber cell. Their formation abolishs the denucleation process and causes lens posterior rupture. These data reveal a novel mechanism of mutant γ-crystallins that involves nuclear targeting and disrupts nuclear functions (Sandilands et al., 2002; Wang et al., 2007b). In another Grygb-I4F mutant line *Clapper* that our laboratory has studied, the inclusions contained α-crystallins and γ-crystallins cause light scattering opacities in the lens. The γB-I4F-crystallin is a denatured protein and binds to α-crystallins which are well-known as molecular chaperones. *In vitro*, recombinant mutant γB-I4F is less heat stable and forms aggregation with α-crystallins (Liu et al., 2005). In a recent study, human deletion mutations W156X in GRYGD and W157X in human GRYGC cause remarkable reduction in solubility, which is probably due to a greater degree of surface hydrophobicity than the wild-type protein (Talla et al., 2008).

In the following chapter, a new mouse nuclear cataract was identified to be linked to a novel mutation of γB-crystallin gene. Investigation of this mutant model revealed a new mechanism to lead to nuclear cataract formation.

Chapter 2 Nuclear Cataract in γB-crystallin S11R Mutation

2.1 Preface of Chapter

This chapter describes the identification of the causative gene mutation for a new dominant cataract in mice and the investigation of the molecular basis for how the mutated gene leads to a dense nuclear cataract.

Genome-wide linkage analysis and DNA sequencing were used to determine the γB-crystallin S11R Mutation. Histology, immunohistochemistry, and Western blotting were used to characterize lens phenotypes. Ion concentrations were measured by an inductively coupled plasma–optical emission spectrometer (ICP-OES).

A point mutation (A to C) of the γB-crystallin gene, which results in the γB-S11R mutant protein, was identified in this cataractous mouse line. Homozygous mutant mice developed dense nuclear cataracts associated with disrupted inner lens fiber cells. Immunohistochemistry data revealed γ-crystallin aggregates at the cell boundaries of inner mature fibers that lose actin filaments. Western blotting showed an increased degradation of crystallin proteins correlated with the nuclear cataract. ICP-OES confirmed a substantial elevation of calcium concentration in mutant lenses.

This dominant cataract was caused by the γB-S11R mutation. Mutant γB-S11R proteins triggered the γ-crystallin aggregation that probably disrupted membrane-cytoskeleton structures of inner fiber cells, causing increased calcium influxes. Subsequent activation of calcium-dependent protein degradation and degeneration of inner mature fiber cells led to the dense nuclear cataract.

2.2 Introduction

The eye lens is composed of lens cells wrapped by a collagen-based membrane, known as the lens capsule. Lens cells are predominantly elongated fiber cells covered by a monolayer of epithelial cells at the surface of the anterior hemisphere (Piatigorsky, 1981). Lens inner fiber cells are mature fibers that lack intracellular organelles to minimize light scattering. Thus, only anterior surface epithelial cells and newly differentiated fiber cells in the lens periphery contain intracellular organelles, such as the endoplasmic reticulum, Golgi, and mitochondria; those cells are able to synthesize proteins or metabolites that maintain the homeostasis of organelle-free inner fiber cells. Several studies have begun to unravel some insights about fiber cell maturation (Bassnett and Mataic, 1997; Nakahara et al., 2007; Nishimoto et al., 2003).

Crystallin proteins (α, β and γ classes) account for more than 90% of total lens proteins (Bloemendal et al., 2004). Lens transparency is suggested to rely on a short-range order of lens crystallin proteins (Delaye and Tardieu, 1983). It is speculated that different crystallin isoforms are needed for the appropriate arrangement of the interfaces of membrane and cytoskeleton in lens fiber cells to ensure transparency and a high refractive index. Alpha-crystallins, consisting of αA and αB subunits, are members of the small heat shock protein family and have chaperone-like activity that prevents the aggregation of denatured proteins *in vitro* (Derham and Harding, 1999; Horwitz, 1992, 2003). Beta- and γ-crystallins are structural proteins that share a common Greek-motif and are extremely heat-stable (Slingsby and Clout, 1999). Beta-crystallins form dimers and higher oligomers while γ-crystallins exist as monomers in the lens. Different γ-crystallin isoforms account for about one third of total lens proteins (Bloemendal et al., 2004). Identification of γN-crystallin suggests an evolutionary link between β- and γ-crystallins (Wistow et al., 2005). It is unknown whether β- and γ-crystallins play active roles in various cellular processes during differentiation and maturation of lens fiber cells. However, it is important to note that these crystallins are expressed in other tissues besides the lens, suggesting that they may have other functions (Andley, 2007).

Gamma-crystallin isoforms A-F show about 77-97% identity at the protein level (Wistow et al., 2005). Studies of recombinant, native and mutant γ-crystallins have demonstrated significant variation in phase separations of different γ-crystallin isoforms and have provided some insights to explain how different γ-crystallin isoforms contribute to “cold cataracts” induced by lower temperature (Clark and Clark, 2000; Lo, 1989; Siezen et al., 1985; Wang et al., 2007a). Mutations that affect the stability and solubility of γ-crystallins can lead to cataracts in humans and mice (Liu et al., 2005; Pande et al., 2005), and some new studies suggest that γ-crystallins may have other important roles in the lens besides acting as passive structural components (Andley, 2007; Wang et al., 2007a).

Here we report a severe nuclear cataract caused by a new point mutation of γB-crystallin. We have found that this mutation specifically alters the subcellular distribution of γ-crystallin in mature fiber cells and leads to unique cellular and biochemical changes that result in a dense

nuclear cataract. This work provides some new information about how γB-crystallin is needed for the appropriate subcellular arrangement of proteins in lens mature fiber cells.

2.3 Methodology and Materials

2.3.1 Mouse Breeding of γB-crystallin S11R Mutant Strain

Mouse care and breeding were performed according to the Animal Care and Use Committee (ACUC)-approved animal protocol (UC Berkeley) and the ARVO Statement for the Use of Animals in Ophthalmic and Vision Research. Mouse pupils were dilated with 1% atropine and 1% phenylephrine before the eyes were examined for lens clarity by a slit lamp.

A spontaneous mouse mutant line (Nm3062) in the A/J strain background was found in the Jackson Laboratory (Bar Harbor, Maine). A γB-S11R mutation was identified in this dominant cataractous mutant line. Original A/J γB-S11R homozygous mice were crossed with C57BL/6J wild-type mice to generate heterozygous mice. Heterozygous mice were then intercrossed to have mixed background wild-type, heterozygous and homozygous mice.

2.3.2 Mouse Genotyping

A small piece of mouse tail was collected according to the animal protocol. Lysis beffer (100 mM Tris pH 8.0, 5 mM EDTA, 0.2% SDS and 200 mM NaCl) with proteinase K was added to dissolve the tail by shaking at 55^0C. An equal amount of isopropanol was used to precipitate DNA. The DNA pellet was then rinsed with 70% ethanol and dissolved in TE buffer (10 mM Tris-Cl pH 7.5 and 1 mM EDTA). A standard PCR protocol was used for genotyping PCR. The γB-S11R mutant allele can be genotyped by using satellite marker D1Mit156 (left: TCTGCTGCCACTTCTGAGAA; right: TGTGTGTCTATGGACATGGATG).

2.3.3 Fresh Lens Imaging

Mice were euthanized by CO2 asphyxiation according to the ACUC-approved animal protocol. Fresh lenses, dissected from enucleated eyeballs, were immediately immersed in PBS at 37°C. Fresh lenses were imaged under a Leica MZ16 dissecting scope using a digital camera.

2.3.4 Histology

Enucleated eyeballs opened at the anterior chamber or posterior vitreous were immersed in a fixative solution containing 2% glutaraldehyde and 2.5% formaldehyde in 0.1 M cacodylate buffer (pH 7.2) at room temperature for 5 days. Samples were postfixed in 1% aqueous OsO4 and then dehydrated through graded acetone. Samples were embedded in eponate 12-araldyte 502 resin (Ted Pella, Redding, CA). Lens sections (1 μm thick) across the equatorial plane were collected on glass slides and stained with toluidine-blue. Bright-field images were acquired through a light microscope (Axiovert 200; Carl Zeiss, Oberkochen, Germany) with a digital camera.

2.3.5 Immunohistochemistry and Confocal Microscopy

Mouse eyes were fixed with fresh 4%formaldehyde in phosphate-buffered saline (PBS) for 30 min, then washed with PBS twice, and soaked overnight in 30% sucrose in PBS. Afterward, the samples were processed by using a standard frozen-section method (Leica, Cryostat 1900, Germany). Tissue sections were washed with three exchanges of sterile PBS (10 min each), followed by blocking (3% BSA, 3% NGS, 0.01% Triton X-100 in PBS) for 1h at room temperature. Antigens were labeled using primary antibodies for 1h at room temperature (or overnight at 4 ^{0}C). After three more washes with sterile PBS, samples were incubated with secondary antibodies (Invitrogen, Carlsbad, CA) for 1h at room temperature. Slides were then mounted with Vectashield Mounting Medium with DAPI (Vector Laboratories, Burlingame, CA). The distributions of antigen were analyzed by laser a confocal microscope (Leica, Wetzlar, Germany).

2.3.6 Western Blot Analysis

Lens total proteins were prepared by homogenizing enucleated fresh lenses that were weighed and homogenized directly in the sample buffer (60 mM Tris, pH 6.8, 2% SDS, 10% glycerol, 5% β-mercaptoethanol, and 0.001% bromophenol blue). To prepare the NaOH-insoluble protein samples, two frozen lenses were homogenized in 0.1 M NaCl and 50 mM Na_2HPO_4 (pH 7) at 40 mg lens wet weight/ml solution. The insoluble material was collected after centrifugation at 15,000 rpm for 15 min and washed once with the same solution. The insoluble pellet was further homogenized in 0.5 ml of 20 mM NaOH, 1 mM $NaHCO_3$ solution. Again, an insoluble pellet was collected after centrifugation at 15,000 rpm for 15 min and washed once with 20 mM NaOH, 1 mM $NaHCO_3$ solution. This insoluble pellet was dissolved in a sample buffer. Equal volumes of samples were loaded on a 12.5% SDS-PAGE gel for separation, and separated proteins were transferred to a polyvinylidene difluoride membrane (Bio-Rad, Hercules, CA). Lens crystallin and connexin proteins were detected by Western blotting with rabbit polyclonal antibodies against α- and γ-crystallins (generously provided by Joseph Horwitz at the University of California, Los Angeles), β-crystallin (generously provided by J. Samuel Zigler at the National Eye Institute), α3- and α8-connexins, and a mouse monoclonal antibody against β-actin (Sigma, St. Louis, MO). More than three sets of lens protein samples of different mice were examined, and representative data were shown.

2.3.7 Ion Concentration Measurement

Lens ion concentration was measured by inductively coupled plasma–optical emission spectrometry (ICP-OES) from a core facility at the University of California, San Diego. The method was described previously. 20 lenses were dissected from postnatal day (P)10 wild-type, heterozygous and homozygous mutant mice and then immediately subjected to vacuum drying for 48 hours. Dry lenses were weighed and solubilized in 500 μL nitric acid (33.5~35%; Fisher Scientific, Pittsburgh, PA) for 12 hours at 37°C with shaking and then diluted with water into 3 mL. Samples were further diluted to reach ion concentrations of 20 ppb to 1 ppm for measurement. According to the estimated sample ion concentration, a series of standards were made. Ion concentrations were determined by their intensities acquired by the instrument. Measurement error was approximately 3%. Ion concentrations were normalized by lens dry weight.

2.3.8 Statistical Analysis

If comparing two groups, Student's t-Test was used. P values < 0.05 were considered significant.

2.4 Results

2.4.1 Identification of γB-crystallin S11R Point Mutation

We identified a dominant cataract from a spontaneous mouse mutant line (*Nm3062*) in the A/J strain background by slit lamp examination. Heterozygous mice displayed hazy nuclear cataracts while homozygous mice developed dense nuclear cataracts at weaning age (Figure 2). Further examination of enucleated fresh lenses revealed that this nuclear cataract could be obviously visualized in mutant mice at the age of postnatal day 7 (P7), but not at postnatal day 1 (P1). Mutant lenses also displayed a unique ring-like structure, located at about 220-350μm away from the lens capsule, which caused abnormal light scattering. Homozygous mutant mice developed dense nuclear cataracts with full penetrance in the A/J strain background or in mixed strain backgrounds including C57BL/6J or 129 strains.

Fifty-four backcross mice between *Nm3062* mutant and wild-type CAST/Ei mice were phenotyped and genotyped for genome-wide linkage analysis. This mutation was mapped to a region between the D1Mit19 and D1Mit21 markers on mouse chromosome 1. A cluster of γ-crystallin genes (*CrygA* to *F*) was located in this region.

DNA sequence analysis of these γ-crystallin genes verified an A to C point mutation of the 11^{th} codon of *Crygb*, which resulted in a substitution of serine with arginine at that codon in γB-crystallin (γB-S11R) (Figure 3). No mutation was detected in other γ-crystallin genes.

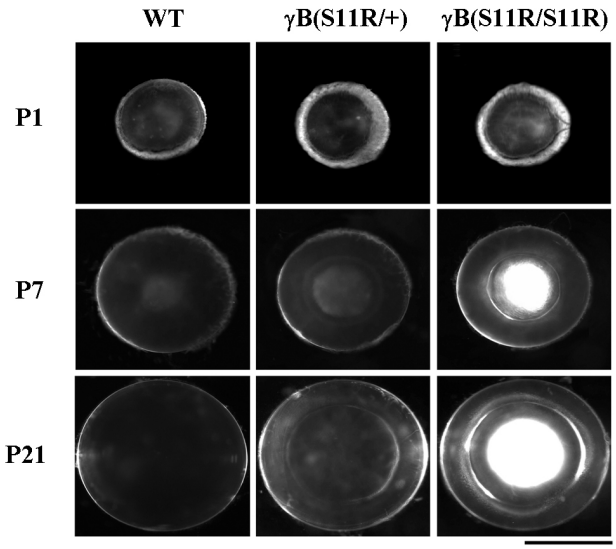

Figure 2. A dominant nuclear cataract linked to the γB-S11R mutation. Lens pictures of wild-type, heterozygous (heter), and homozygous (homo) mutant mice at P1, P7, and P21. Images were taken of enucleated fresh lenses immersed in PBS at 37°C. Scale bar, 1 mm.

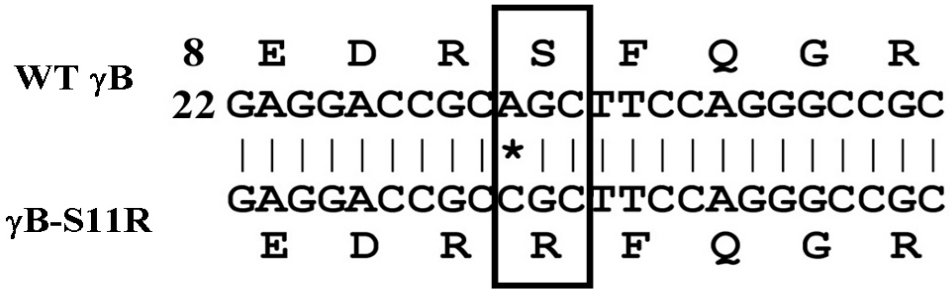

Figure 3. DNA sequencing data verified an A-to-C mutation in the Crygb gene. This point mutation resulted in a substitution of the serine residue by an arginine at the 11th codon of the γB-crystallin protein (γB-S11R).

2.4.2 Histology Reveals Normal Peripheral Fiber Cells and Disintegrated Inner Fiber Cells

Toluidine-blue stained lens histology sections were prepared from neonatal mice (Figure 4A). These histological sections showed that peripheral fibers developed normally at the bow region of P3 mutant lenses. However, inner fiber cells of both heterozygous γB(S11R/+) and homozygous γB(S11R/S11R) lenses displayed uneven toluidine-blue staining with abnormal darkly-stained areas. Disintegrated fiber cells appeared only in the core of homozygous γB(S11R/S11R) lenses while lens peripheral fiber cells displayed relatively normal morphology.

The periphery of γB(S11R/S11R) mutant lenses remained transparent even in older mice (Figure 2). Representative histological data of lens peripheral fibers between wild-type and γB(S11R/S11R) mutant mice at the age of postnatal day 21 were shown (Figure 4B). Lens cross-sections revealed that peripheral fiber cells of P21 γB(S11R/S11R) lenses remained relatively normal similar to those of P21 wild-type lenses. Therefore, histological data confirmed that altered inner fiber cells were correlated to the nuclear cataract phenotype caused by the γB-S11R mutation.

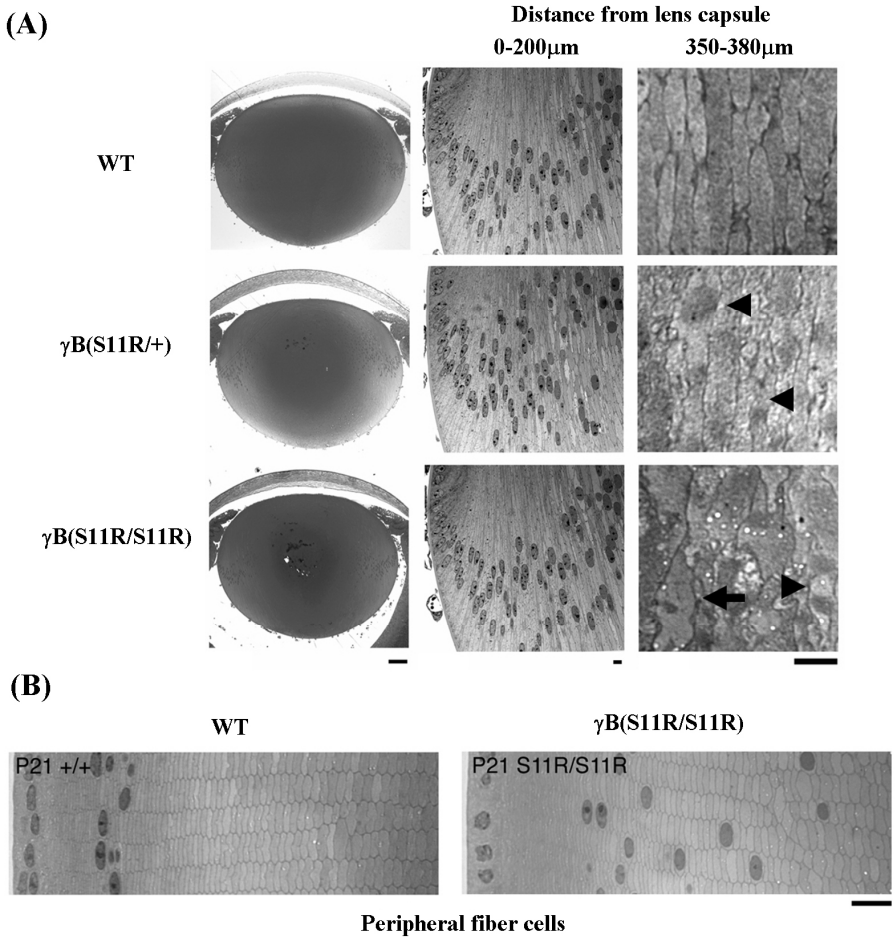

Figure 4. Histology of P3 and P21 wild-type and γB-S11R mutant lenses. (**A**, *left*) P3 whole lens sections. Scale bar, 100 μm. *Right*: high-magnification images of lens bow and inner regions. Bow regions of wild-type (WT) and mutant lenses displayed normal morphology. However, inner regions of γB(S11R/+) and γB(S11R/S11R) lenses displayed uneven staining (*arrowheads*), and only γB(S11R/S11R) lenses revealed disintegrated fiber cells (*arrow*). (**B**) Lens cross-sections revealed that peripheral fiber cells of P21 γB(S11R/S11R) lenses remained relatively normal, similar to those of P21 wild-type lenses. Scale bars: (**A**) 10 μm; (**B**) 20 μm.

2.4.3 Gamma-crystallin Aggregates Appear Adjacent to the Cell Boundary and F-actin Disappears in Inner Fiber Cells

Based on the fact that the γB-S11R mutation leads to a dense nuclear cataract that is different from the lamellar cataract caused by the γB-I4F mutation as reported previously (Liu et al., 2005), we hypothesize that, unlike γB-I4F, γB-S11R mutant proteins trigger a unique event to disrupt inner fiber cells to cause nuclear cataracts. To evaluate this hypothesis and to understand how mutant proteins lead to the disruption of inner fiber cells in γB(S11R/S11R) lenses, we examined the cellular distribution of γ-crystallins in lens fiber cells of both wild-type and mutant lenses. Gamma-crystallins account for about one third of total proteins in lens fibers. Immunostaining of γ-crystallin revealed uniformly distributed signal in both peripheral and interior fiber cells of wild-type lenses (Figure 5A). Gamma-crystallins were also uniformly stained in peripheral fiber cells of γB(S11R/S11R) mutant lenses. However, γ-crystallin aggregates were detected adjacent to the cell boundary of inner fibers and were segregated from actin filaments (Figure 5A). Further studies of P7 and P21 γB(S11R/S11R) lenses revealed that actin filaments completely disappeared in inner fiber cells starting at about 220-350μm away from the lens capsule (Figure 5B). Thus, these results indicate that γB-S11R mutant proteins lead to the formation of unique γ-crystallin aggregates and the disruption of actin filaments in inner fiber cells. The loss of F-actin staining in the lens section (Figure 5B) seems to be correlated with the appearance of the abnormal ring, peripheral to the dense nuclear cataract in γB(S11R/S11R) lenses (Figure 2).

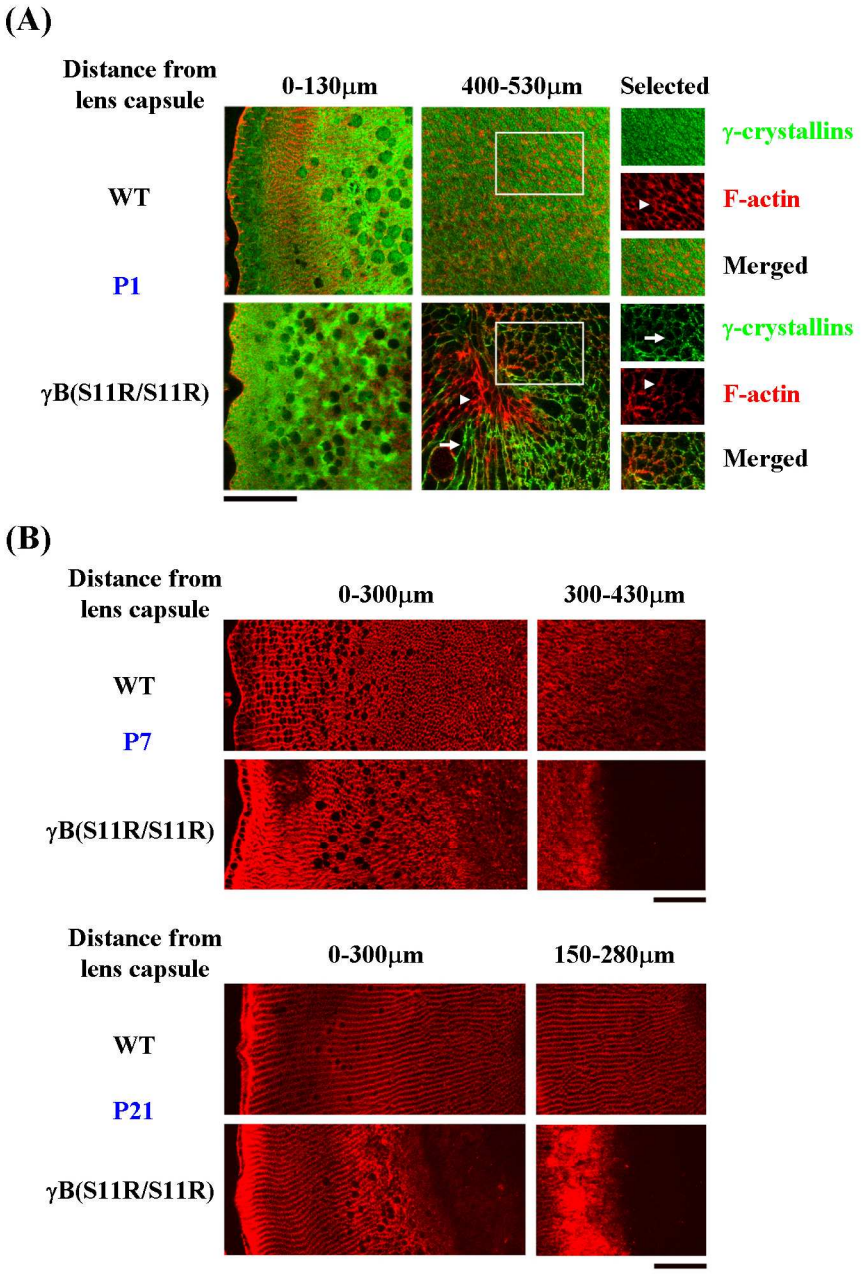
(A)
Distance from lens capsule
0-130μm
400-530μm
Selected
γ-crystallins
F-actin
Merged
WT
P1
γB(S11R/S11R)
γ-crystallins
F-actin
Merged
(B)
Distance from lens capsule
0-300μm
300-430μm
WT
P7
γB(S11R/S11R)
Distance from lens capsule
0-300μm
150-280μm
WT
P21
γB(S11R/S11R)

Figure 5. Immunostaining of γ-crystallins and actin filaments in lens fiber cells. (**A**) P1 wild-type and homozygous γB(S11R/S11R) lens frozen sections were stained with anti–γ-crystallin antibody (*green*) and rhodamine-phalloidin (*red*). *Boxes*: selected areas that show separated and merged fluorescent images of γ-crystallin and F-actin in lens inner fiber cells. *White arrows*: γ-Crystallin aggregates adjacent to cell boundaries. *White arrowheads*: F-actin. (**B**) Rhodamine-phalloidin–stained frozen sections of P7 and P21 wild-type and γB(S11R/S11R) lenses. Actin filaments disappeared in inner fiber cells of γB(S11R/S11R) mutant lenses, starting at approximately 350 μm from the lens capsule in the P7 sample and approximately 200 μm in the P21 sample (*white arrowheads*). Scale bars, 50 μm.

2.4.4 Nuclear Cataracts are Associated with the Degradation of Crystallin Proteins

Morphological data suggest that dense nuclear cataracts are associated with disintegrated inner fiber cells. In order to determine whether or not protein degradation occurred in these disintegrated lens fiber cells, we analyzed crystallins in wild-type and mutant lenses by Western blotting. Cleaved forms of different crystallins (αA, αB, β and γ) were detected in P21 mutant lenses but not in wild-type lenses. Moreover, cleaved αB- and γ-crystallins were detected in P7 mutant lenses (Figure 6). Homozygous mutant lenses contained more cleaved crystallins than heterozygous mutant lenses. There was no detectable cleavage of αB-crystallin in P1 mutant lenses (data not shown). Thus, these Western blotting results indicated that the severity of the nuclear cataract was associated with the amount of cleaved crystallins (α and β/γ) in mutant lenses.

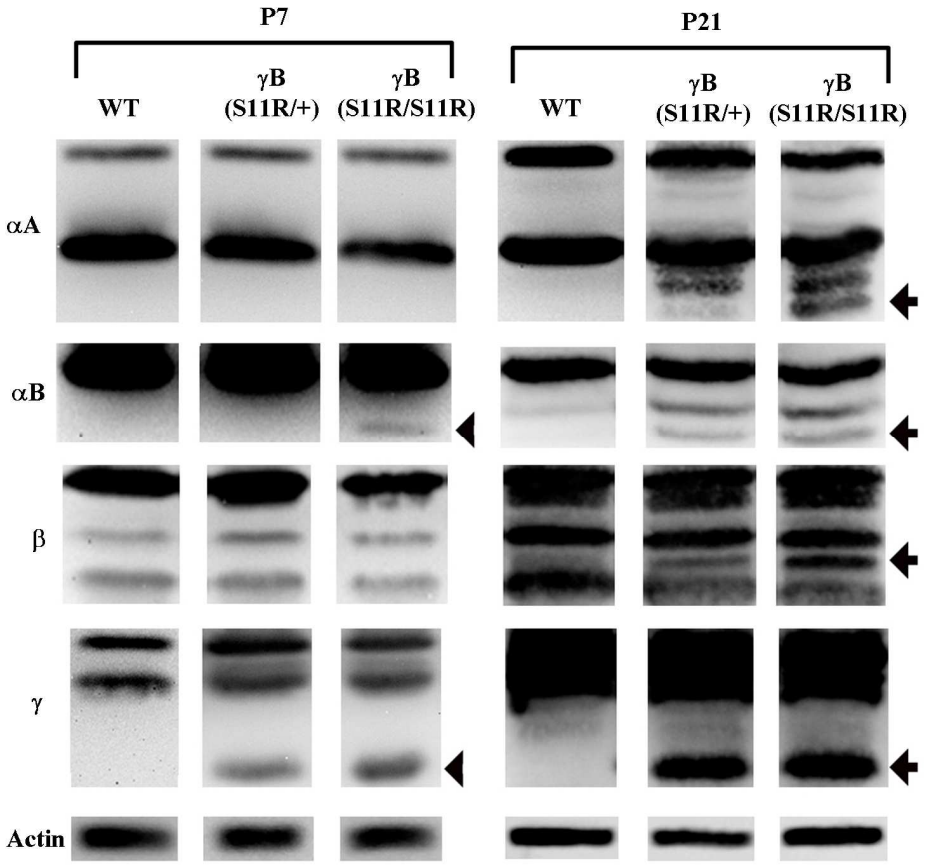

Figure 6. Western blotting of lens crystallin proteins. Compared with wild-type (WT) lenses, cleaved αB- and γ-crystallins were detected in P7 mutant lenses (*arrowheads*). In P21 mutant lenses, cleaved forms of all crystallins (αA, αB, β, γ) were detected (*arrows*). Total amount of β-actin remained unchanged between P7 and P21 wild-type and mutant lenses.

2.4.5 Calcium Concentration Is Elevated in Mutant Lenses

An activation of calcium-dependent proteases in mouse lenses often results in crystallin degradation. An influx of extracellular calcium into inner fiber cells could activate calcium-dependent proteases. We hypothesize that elevated calcium levels lead to increased crystallin degradation, resulting in severe nuclear cataracts in γB(S11R/S11R) mutant lenses. Therefore, we examined the total amount of ions, including calcium, magnesium, sodium and potassium, in lenses by ICP-OES. The total calcium level was increased about 4-fold in γB(S11R/S11R) lenses compared to wild-type lenses while sodium, magnesium and potassium levels were only slightly increased in γB(S11R/S11R) lenses. Calcium concentration was also increased in heterozygous γB(S11R/+) mutant lenses (Figure 7). This result confirmed that crystallin degradation likely resulted from an activation of calcium-dependent proteases in γB-S11R mutant lenses. Furthermore, the amount of calcium elevation and cleaved crystallins was correlated with the severity of the nuclear cataract in γB-S11R mutant lenses.

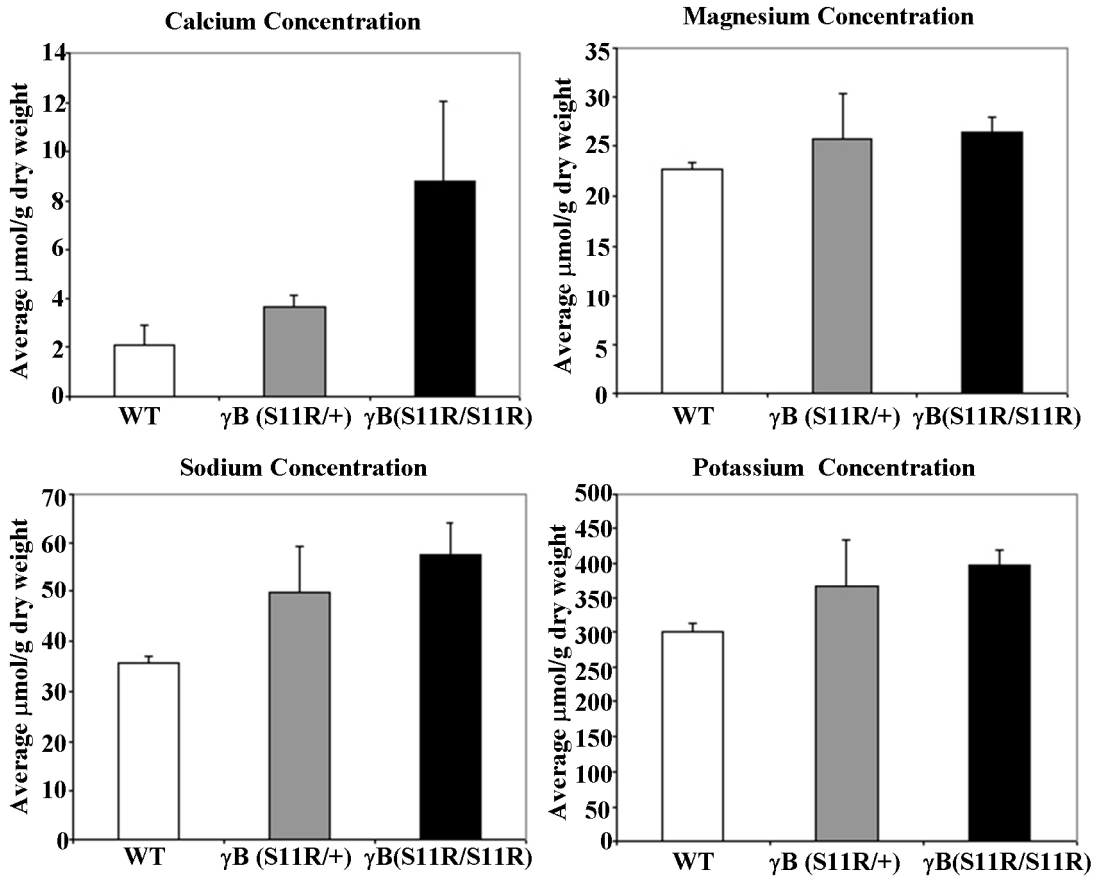

Figure 7. Total amounts of calcium, magnesium, sodium, and potassium in the lens measured by ICP-OES. Compared with WT lenses, calcium concentration was slightly increased in γB(S11R/+) lenses; total calcium level was increased approximately fourfold in γB(S11R/S11R) lenses, whereas sodium, magnesium, and potassium levels were only slightly increased. These differences were statistically significant ($n = 3$; $P < 0.05$).

2.5 Discussion

2.5.1 Summary

This work provides at least part of the molecular mechanism for how the γB-S11R mutation leads to a nuclear cataract. Histological and biochemical data indicate that the dense nuclear cataract caused by this mutation is related to the degeneration of inner fiber cells. Fiber cell degeneration is correlated with an increase of cleaved crystallin proteins and a disruption of actin filaments. Specific aggregation of γ-crystallins in γB-S11R mutant lenses is likely to be one of the early events that trigger downstream changes such as the loss of actin filaments and the elevation of calcium concentration. Activation of calcium-dependent proteases and disruption of cytoskeletal structures directly contribute to the degeneration of inner fiber cells, which lead to severe nuclear cataracts. However, some important questions remain to be answered: 1) how do γB-S11R mutant proteins cause aggregation of γ-crystallins adjacent to the cell boundary of inner mature fiber cells; 2) what leads to elevated calcium concentration; and 3) how do actin filaments undergo disassembly. One possible explanation is that γ-crystallin aggregates disrupt or damage membrane-cytoskeletal structures to increase the influx of extracellular calcium, and elevated intracellular calcium subsequently activates calcium-dependent proteases, such as calpains, leading to crystallin degradation.

2.5.2 Implications of Experimental Results

Gamma-crystallin mutations are one of the most common causes of hereditary cataracts in humans and mice (Bloemendal et al., 2004). Studies of several mutant γ-crystallin proteins suggest that a decrease in the stability and/or solubility of mutated proteins facilitate abnormal protein aggregates in the cytosol of fiber cells to cause distinct cataracts, such as "crystal-like" or lamellar cataracts (Evans et al., 2004; Fu and Liang, 2002; Liu et al., 2005; Pande et al., 2001). We and other investigators have also found that mutant γ-crystallin proteins can form nuclear aggregates in differentiating fiber cells to inhibit the denucleation process leading to severe cataracts with ruptured lenses in mice (Sandilands et al., 2002; Wang et al., 2007a). The γD-P23T crystallin mutation leads to various types of cataracts in humans (Mackay et al., 2004; Nandrot et al., 2003; Shentu et al., 2004). Therefore, nonspecific protein aggregation of mutated γ-crystallin proteins with reduced solubility and/or stability is not sufficient to explain how different types of cataracts can result from one particular mutation. Our experimental evidence suggests that mutated γ-crystallin proteins may perturb other specific protein-protein interactions or important cellular events during fiber cell maturation that lead to distinct types of cataracts. Different types of cataracts often result from a combination of a specific gene mutation and other genetic modifier(s) (Gong et al., 1999; Nag et al., 2007; Wang et al., 2007a).

The distribution of wild-type or mutant γB-crystallin proteins in the mouse lens has not been precisely determined. The γB-crystallin transcript is predominantly expressed in lens fibers, and the proportion of γB (and γC) proteins is reduced in the lens as mice age (Murer-Orlando et al., 1987; Ueda et al., 2002). The γB-I4F mutant protein is less heat-stable *in vitro*, binds to α-crystallin in lens homogenates and forms cytosolic aggregates *in vivo* (Liu et al., 2005). The γB-I4F mutation results in a lamellar cataract (from lens deep cortex to the nucleus) while the γB-S11R mutation causes an abnormal cortical ring and a dense nuclear cataract. Therefore, γB-crystallin is likely to be highly synthesized in differentiated fiber cells of the deep cortex. These two point mutations likely perturb the properties and/or functions of γB-crystallin in different ways. We predict that additional factors, present only in mature fiber cells of lens nucleus, are required for γB-S11R mutant proteins to trigger γ-crystallin aggregation adjacent to the cell boundary and to disrupt calcium homeostasis and the cytoskeleton in inner mature fiber cells.

Calcium homeostasis is crucial for lens transparency in humans and rodents (Duncan and Wormstone, 1999; Truscott et al., 1990). Mouse lenses are even more sensitive to calcium levels due to the presence of calcium-dependent proteases, such as calpains, especially the calpain 3 isoform (Lp82) (Azuma et al., 1997; Nakamura et al., 2000; Tang et al., 2007). Elevated intracellular calcium levels activate calpains that cleave α-, β- and γ-crystallin proteins (Tang et al., 2007; Ueda et al., 2002; Xia et al., 2006a). It is interesting to note that the γB-S11R mutation disrupts calcium homeostasis in the lens and causes activation of calcium-dependent degradation of crystallin proteins. Although β- and γ-crystallins lack a typical calcium binding site, recent studies suggest that the Greek key motif is directly involved in calcium binding *in vitro* (Jobby and Sharma, 2007; Rajini et al., 2003; Rajini et al., 2001). It is unclear whether γ-crystallin

proteins regulate intracellular calcium level in lens fiber cells. However, it is important to further investigate how the γB-S11R mutation perturbs calcium homeostasis in the lens (Gao et al., 2004; Mathias et al., 1997).

2.5.3 Future Directions

In summary, this work further supports the new hypothesis that mutant crystallins can cause cataracts by selectively perturbing protein-protein interactions, distinct cellular events during fiber cell maturation and/or specific cellular structures of lens mature fibers. This differs from an old hypothesis that cataracts result from light scattering caused by high molecular weight aggregates formed by mutant proteins. However, it is unclear whether or not γB-S11R affects self protein-protein interactions and/or its interactions with other proteins in the lens. Further studies such as characterization of the solubility and stability of its recombinant proteins *in vitro*, determination of subcellular distribution of γB-S11R protein in transfected cells and identification of γB-S11R interacting factor(s) may provide additional mechanistic information to explain the differences between γB-S11R and γB-I4F mutations and/or to elucidate the intermediate steps for how γB-S11R mutant proteins lead to nuclear cataracts.

Chapter 3 Alpha3 Connexin Mediated Prevention of Nuclear Cataract

3.1 Preface of Chapter

This chapter describes the studies of a new approach through elevated gap junction communication to suppress the dominant cataract caused by the γB-crystallin S11R point mutation. Mutant γB-S11R proteins induce abnormal protein aggregation that probably disrupts membrane-cytoskeleton structures of inner fiber cells. Subsequently increased calcium influx and activation of calcium-dependent protein degradation lead to the degeneration of inner mature fiber cells and a dense nuclear cataract. Increased calcium level and activation of calcium-dependent protein degradation also occur in the nuclear cataract of α3 knockout lenses. Thus, similar mechanisms are associated with nuclear cataracts caused by the γB-S11R point mutation or the α3 connexin null mutation. Moreover, knock-in α3 connexin (Ki), α8 connexin (Cx50) replaced with α3 connexin (Cx46) in α8 gene locus, reduces the calcium level in the lens. Thus, we have generated Ki γB-S11R double compound mutant mice to investigate whether knock-in α3 connexin can inhibit cataract formation caused by the γB-S11R mutation. α8(Ki/Ki) γB(S11R/S11R) double homozygous compound mutant mice have relatively clear lenses with well-organized fiber cells up to one year old (the oldest age examined so far). Immunohistochemistry data reveal that γ-crystallin proteins mainly stay in the cytosol of inner mature fibers with normal actin filaments. No obvious degradation of crystallin proteins is detected by Western blotting and calcium concentrations of compound mutant lenses are similar to wild-type lenses. Moreover, one allele of knock-in α3 only delays the onset of cataract formation. α8(Ki/-) α3(-/-) γB(S11R/S11R) compound mutant mice have cataracts with variable opacities at weaning age. The mechanism for the dosage-dependent inhibition of this nuclear cataract needs to be further elucidated.

In conclusion, we believe that knock-in α3 connexin probably enhances the intercellular cell-cell communication and adhesion in the lens, which in turn prevents calcium elevation from facilitating calcium-dependent protein degradation, thus preserving normal fiber cell morphology and preventing the degeneration of inner fiber cells.

3.2 Introduction

The ocular lens is an avascular organ that needs to maintain life-long transparency. However, organelle-free mature fiber cells lack stress resistance and protein turnover machinery. Any small disturbances of the system, such as osmotic pressure change and abnormal protein modification, may lead to cataract formation. Non-surgical prevention of age-related cataract or congenital cataract remains a challenging topic due to the impression that cataract is irreversible, and that it may be impossible to prevent cellular disruptions or abnormal protein aggregations caused by denatured or mutant proteins.

Gap junction channels play important roles in regulating lens homeostasis by providing low-resistance pathways for both electrical signals and small metabolic substrates between lens cells. Distinct and redundant expressions of three connexin isoforms compose gap junction channels in the lens: The α1 connexin gene is specifically expressed in lens epithelial cells, the α3 connexin is mainly found in lens fiber cells, and the α8 connexin gene is expressed in both epithelial cells and fiber cells. Genetic studies of α3 and α8 connexins have demonstrated the importance of their roles in maintaining lens transparency and proper lens growth. Null mutation of the α3 connexin gene resulted in nuclear cataracts in mice (Gong et al., 1997), while the deletion of α8 connexin gene lead to cataracts and smaller lenses (Rong et al., 2002). Moreover, genetic replacement of endogenous α8 connexin with wild-type α3 connexin by homologous recombination rescued lens clarity but did not restore the reduction in lens size caused by the absence of α8 (White, 2002). In addition, heterozygous replacement of α8 with wild-type α3 rescued growth defect but produced lens opacity due to a biochemical coupling alteration. Moreover, homozygous knocked-in wild-type α3 connexin, but without endogenous α3 connexin, was sufficient to maintain lens transparency (Martinez-Wittinghan et al., 2003). Unpublished works from our laboratory suggest that heterozygous knocked-in α3 connexin without any endogenous α3 and α8 connexin was able to make clear lenses. Knock-in α3 connexin could also prevent severe cataracts caused by a α8-G22R mutation (Xia et al., 2006b).

The γB-crystallin S11R point mutation caused dominant cataracts in mice as the previous chapter describes (Li et al., 2008). Homozygous γB(S11R/S11R) mice developed dense nuclear cataracts resulting from disrupted inner fibers and calcium-dependent protein degradation. Reduced levels of endogenous α3 and α8 subunits were detected in the lenses of γB(S11R/S11R) mice. Knock-in α3 connexin could 1) significantly increase α3 connexin expression; 2) reduce the calcium level in the lens; and 3) enhance coupling and adhesion between fiber cells. Thus, we hypothesize that knock-in α3 connexin can inhibit cataract formation caused by the γB-S11R mutation. To test this hypothesis and to examine the anti-cataract effect of knock-in α3, we have generated double compound mutant mice that express both mutant γB-S11R and knock-in α3 connexin. We have found that the dense nuclear cataract was delayed or rescued. Studies of the morphological and biochemical properties of double compound mutant mice have revealed that improved lens homeostasis by increasing gap junction communication stabilized proteins in the lens core; enhanced cell-cell adhesion by gap junction channels maintained normal cellular

structures and integrity. This work demonstrates the concept that improved lens homeostasis and cell-cell contact can prevent or delay age-related nuclear cataracts.

3.3 Methodology and Materials

3.3.1 Mouse Breeding of α3-connexin Knock-in γB-S11R Compound Mutant Mice

Mouse care and breeding were performed according to the Animal Care and Use Committee (ACUC)-approved animal protocol (UC Berkeley) and the ARVO Statement for the Use of Animals in Ophthalmic and Vision Research. Mouse pupils were dilated with 1% atropine and 1% phenylephrine before the eyes were examined for lens clarity by a slit lamp.

Original γB-S11R homozygous mice were crossed with α3 connexin knock-in homozygous mice. Offspring of α3 connexin knock-in γB-S11R double heterozygous compound mutant mice were intercrossed to generate double homozygous mice α8(Ki/Ki) γB(S11R/S11R). Other two compound mutant mouse lines, α8(Ki/Ki) α3(-/-) γB(S11R/S11R), containing two α3 knock-in alleles, α8(Ki/-) α3(-/-) γB(S11R/S11R), containing only one α3 knock-in allele, without endogenous α3 alleles were generated from several generations of breeding the α8(Ki/Ki) γB(S11R/S11R) with connexin double-knockout α8(–/–) α3(–/–) mice. Intercross of α8(Ki/-) α3(-/-) γB(S11R/S11R) compound mutant mice generated the following three types of littermates: α8(Ki/Ki) α3(-/-) γB(S11R/S11R), α8(Ki/-) α3(-/-) γB(S11R/S11R) and α8(-/-) α3(-/-) γB(S11R/S11R).

3.3.2 Mouse Genotyping

A small piece of mouse tail was collected according to the animal protocol. Lysis buffer (100 mM Tris pH 8.0, 5 mM EDTA, 0.2% SDS and 200 mM NaCl) with proteinase K was added to dissolve the tail by shaking at 55^{0}C. An equal amount of isopropanol was used to precipitate DNA. The DNA pellet was rinsed with 70% ethanol and dissolved in TE buffer (10 mM Tris-Cl pH 7.5 and 1 mM EDTA). The standard PCR protocol was used for genotyping PCR. γB-S11R mutant alleles can be genotyped by using satellite marker D1Mit156 (left: TCTGCTGCCACTTCTGAGAA; right: TGTGTGTCTATGGACATGGATG). The genotyping of the α3 and α8 mutant allele was assessed by PCR as described in previous papers (Gong et al., 1997; Rong et al., 2002; White, 2002).

3.3.3 Fresh Lens Imaging and Light Scattering Quantification

Mice were euthanized by CO2 asphyxiation according to the ACUC-approved animal protocol. Fresh lenses, dissected from enucleated eyeballs, were immediately immersed in PBS at 37°C. Fresh lenses were imaged under a Leica MZ16 dissecting scope using a digital camera. Light scattering in the lenses caused by cataract was measured using the HR 2000CG_UV_NIR High Resolution Spectrometer and a QP400-2-UV-VIS fiber optic cable (400 μm cable diameter) (Ocean Optics, Dunedin, FL). Lenses were illuminated by a white light source perpendicular to the equator of the lens. Scattered light was captured by the optic fiber with a whole acceptance of angle of 24.8°. Spectrums were recorded and saved for later comparison. Each lens was measured twice in succession to show repeatability. The measurements were represented as graphs with wavelength on the x-axis and light intensity on the y-axis. Denser cataracts scattered more light, and thus, the light scattering intensity measured by the detector increased. Measurements were stored as ASCII files, and the area under the curve was calculated by a Matlab program.

3.3.4 Histology

Enucleated eyeballs opened at the anterior chamber or posterior vitreous were immersed in a fixative solution containing 2% glutaraldehyde and 2.5% formaldehyde in 0.1 M cacodylate buffer (pH 7.2) at room temperature for 5 days. Samples were postfixed in 1% aqueous OsO4 and then dehydrated through graded acetone. Samples were embedded in eponate 12-araldyte 502 resin (Ted Pella, Redding, CA). Lens sections (1 μm thick) across the equatorial plane were collected on glass slides and stained with toluidine-blue. Bright-field images were acquired through a light microscope (Axiovert 200; Carl Zeiss, Oberkochen, Germany) with a digital camera.

3.3.5 Immunohistochemistry and Confocal Microscopy

Mouse eyes were fixed with fresh 4%formaldehyde in phosphate-buffered saline (PBS) for 30 min, then washed with PBS twice, and soaked overnight in 30% sucrose in PBS. Afterward, the samples were processed by using a standard frozen-section method (Leica, Cryostat 1900, Germany). Tissue sections were washed with three exchanges of sterile PBS (10 min each), followed by blocking (3% BSA, 3% NGS, 0.01% Triton X-100 in PBS) for 1h at room temperature. Antigens were labeled using primary antibodies for 1h at room temperature (or overnight at 4 ^{0}C). After three more washes with sterile PBS, samples were incubated with secondary antibodies (Invitrogen, Carlsbad, CA) for 1h at room temperature. Slides were then mounted with Vectashield Mounting Medium with DAPI (Vector Laboratories, Burlingame, CA). The distributions of antigen were analyzed by a laser confocal microscope (Leica, Wetzlar, Germany).

3.3.6 Western Blot Analysis

Lens total proteins were prepared by homogenizing enucleated fresh lenses that were weighed and homogenized directly in the sample buffer (60 mM Tris, pH 6.8, 2% SDS, 10% glycerol, 5% β-mercaptoethanol, and 0.001% bromophenol blue). To prepare the NaOH-insoluble protein samples, two frozen lenses were homogenized in 0.1 M NaCl and 50 mM Na_2HPO_4 (pH 7) at 40 mg lens wet weight/ml solution. The insoluble material was collected after centrifugation at 15,000 rpm for 15 min and washed once with the same solution. The insoluble pellet was further homogenized in 0.5 ml of 20 mM NaOH, 1 mM $NaHCO_3$ solution. Again, an insoluble pellet was collected after centrifugation at 15,000 rpm for 15 min and washed once with 20 mM NaOH, 1 mM $NaHCO_3$ solution. This insoluble pellet was dissolved in a sample buffer. Equal volumes of samples were loaded on a 12.5% SDS-PAGE gel for separation, and separated proteins were transferred to a polyvinylidene difluoride membrane (Bio-Rad, Hercules, CA). Lens crystallin and connexin proteins were detected by Western blotting with rabbit polyclonal antibodies against α- and γ-crystallins (generously provided by Joseph Horwitz at the University of California, Los Angeles), β-crystallin (generously provided by J. Samuel Zigler at the National Eye Institute), α3- and α8-connexins, and a mouse monoclonal antibody against β-actin (Sigma, St. Louis, MO). More than three sets of lens protein samples of different mice were examined, and representative data were shown.

3.3.7 Ion Concentration Measurement

Lens ion concentration was measured by inductively coupled plasma–optical emission spectrometry (ICP-OES) from a core facility at the University of California, San Diego. The method was described previously. 20 lenses were dissected from postnatal day (P)10 wild-type, heterozygous and homozygous mutant mice and then immediately subjected to vacuum drying for 48 hours. Dry lenses were weighed and solubilized in 500 μL nitric acid (33.5~35%; Fisher Scientific, Pittsburgh, PA) for 12 hours at 37°C with shaking and then diluted with water into 3 mL. Samples were further diluted to reach ion concentrations of 20 ppb to 1 ppm for measurement. According to the estimated sample ion concentration, a series of standards were made. Ion concentrations were determined by their intensities acquired by the instrument. Measurement error was approximately 3%. Ion concentrations were normalized by lens dry weight.

3.3.8 Statistical Analysis

If comparing two groups, Student's t-Test was used. P values < 0.05 were considered significant.

3.4 Results

3.4.1 A Nuclear Cataract Is Rescued by Knock-in α3 Connexin under α8 Locus

Chapter two reports a dominant nuclear cataract caused by the γB-crystallin-S11R mutation. In γB-S11R lenses, disruption of membrane-cytoskeleton structures and calcium-dependent protein degradation were observed. Similar lens phenotypes and mechanisms are associated with nuclear cataracts caused by the γB-S11R point mutation and the α3 connexin null mutation. Thus, overexpression of α3 connexin by knock-in may restore lens transparency in γB-S11R mutant mice. Ki γB-S11R double compound mutant mice were generated, fresh lens pictures on postnatal day 21 (P21) show that knock-in α3 connexin can inhibit cataract formation caused by the γB-S11R mutation (Figure 8A). Ki/Ki γB(S11R/S11R) lenses were smaller, but no longer developed dense nuclear cataracts up to one year old (data not shown). The small lens phenotype was due to an absence of α8 connexin (Rong et al., 2002). Light scattering measurement of P21 WT, γB(S11R/S11R) and Ki/Ki γB(S11R/S11R) lenses using optic fiber spectrometer indicated that γB(S11R/S11R) lenses exhibited the most dramatic light scattering while the rescue Ki/Ki γB(S11R/S11R) lenses showed minimal amount of light scattering compared to the WT (Figure 8B and 8C).

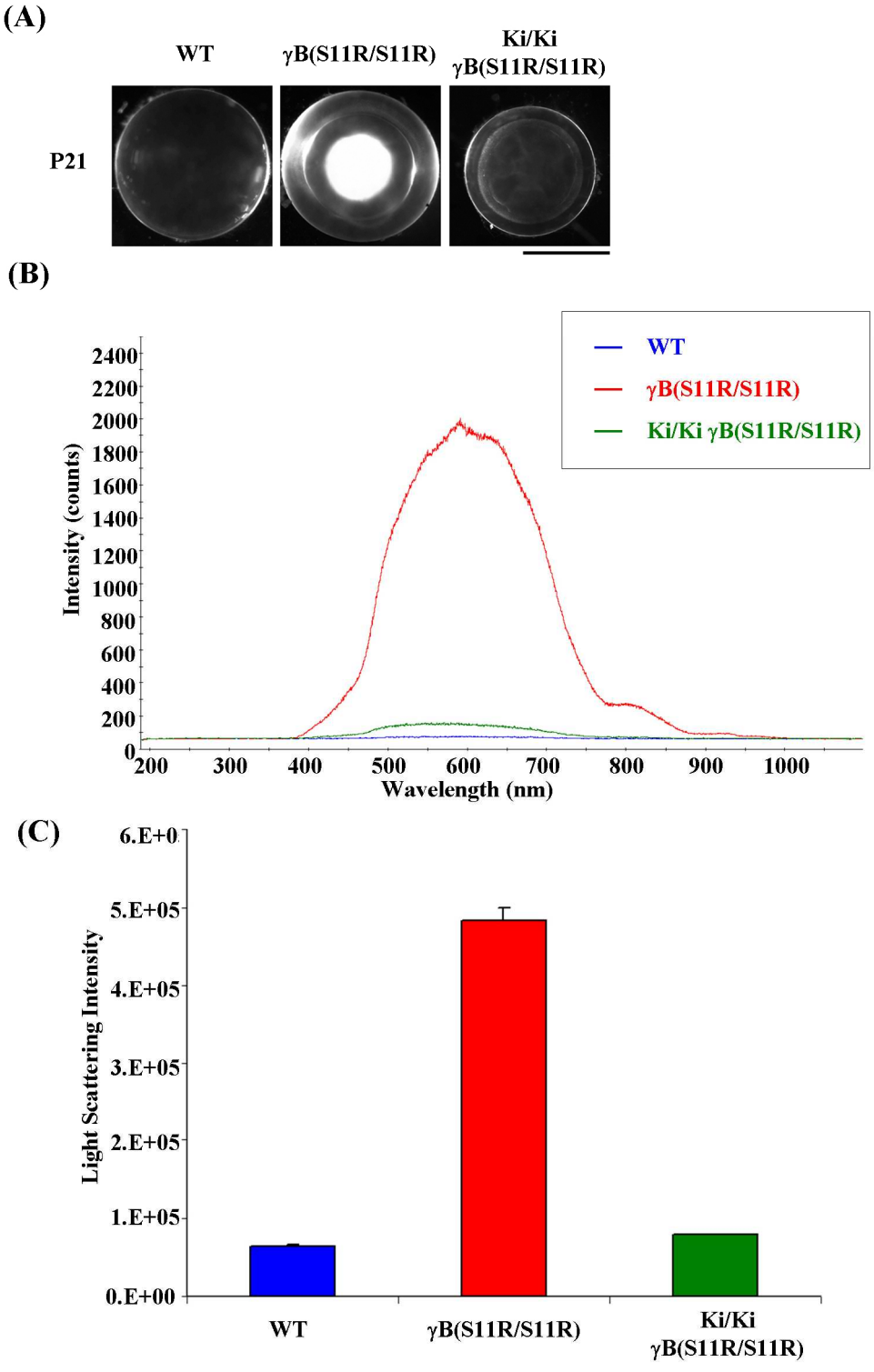
(A)
WT
γB(S11R/S11R)
Ki/Ki γB(S11R/S11R)
P21
(B)
WT
γB(S11R/S11R)
Ki/Ki γB(S11R/S11R)
Intensity (counts)
2400
2200
2000
1800
1600
1400
1200
1000
800
600
400
200
0
200
300
400
500
600
700
800
900
1000
Wavelength (nm)
(C)
Light Scattering Intensity
6.E+0
5.E+05
4.E+05
3.E+05
2.E+05
1.E+05
0.E+00
WT
γB(S11R/S11R)
Ki/Ki γB(S11R/S11R)

Figure 8. A dominant nuclear cataract caused by the γB-S11R mutation was rescued by knock-in α3-connexin. (**A**) Lens pictures of wild-type (WT), γB-S11R homozygous (symbol as γB(S11R/S11R)) and α3-connexin knock-in γB-S11R homozygous compound mutant mice (symbol as Ki/Ki γB(S11R/S11R)) at the age of postnatal day 21 (P21). Images were taken of enucleated fresh lenses immersed in PBS at 37°C. Scale bar, 1mm. (**B**) Light scattering measurement of P21 WT, γB(S11R/S11R) and Ki/Ki γB(S11R/S11R) lenses using optic fiber spectrometer (HR2000CG-UV-NIR, Ocean Optics). Representative graphs of each genotype are shown in the color indicated. γB(S11R/S11R) lenses exhibited the most dramatic light scattering while the rescue Ki/Ki γB(S11R/S11R) lenses showed minimal amount of light scattering compared to the WT. (**C**) The areas under each curve of figure 1b were calculated and plotted as a chart. All differences were statistically significant ($N=4$, $P<0.05$).

3.4.2 Overexpression of α3 Connexin Suppresses Degradation of Crystallin Proteins and Calcium Concentration Is Normal in Knock-in Mutant Lenses

Since α8 connexin locus is replaced by α3 connexin in the knock-in allele, we confirmed by Western blotting that P10 Ki/Ki γB(S11R/S11R) lenses had 3-fold increases of α3 connexin levels compared to the wild-type, and more than 6-fold increases compared to γB(S11R/S11R) homozygous lenses. This suggests that knock-in allele did drive overexpression of α3 connexin. As predicted, α8 connexin band was absent from Ki/Ki γB(S11R/S11R) samples. γB(S11R/S11R) lenses had a significant decrease in the amount of α8 connexin (Figure 9A). Previously, we have observed lens total calcium elevation and calcium-dependent crystallin protein degradation in γB(S11R/S11R) lenses. Because knock-in α3 connexin reduces the calcium level in the lens, we measured the calcium concentration in Ki/Ki γB(S11R/S11R) lenses and calcium concentration of Ki/Ki γB(S11R/S11R) samples was equivalent to the wild-type level (Figure 9B). No obvious calcium-depend protein degradation was observed, γ-crystallin cleavage was detected in P10 Ki/Ki γB(S11R/S11R) rescue lenses (Figure 9C). The γ-crystallin cleavage band might not have any association with cataract phenotypes, since heterozygous γB(S11R/+) and Ki/Ki γB(S11R/S11R) rescue lenses also had this cleavage band (Li et al., 2008). The γ-crystallin cleavage protein amount is also indistinguishable compared to γB(S11R/S11R) before weaning age.

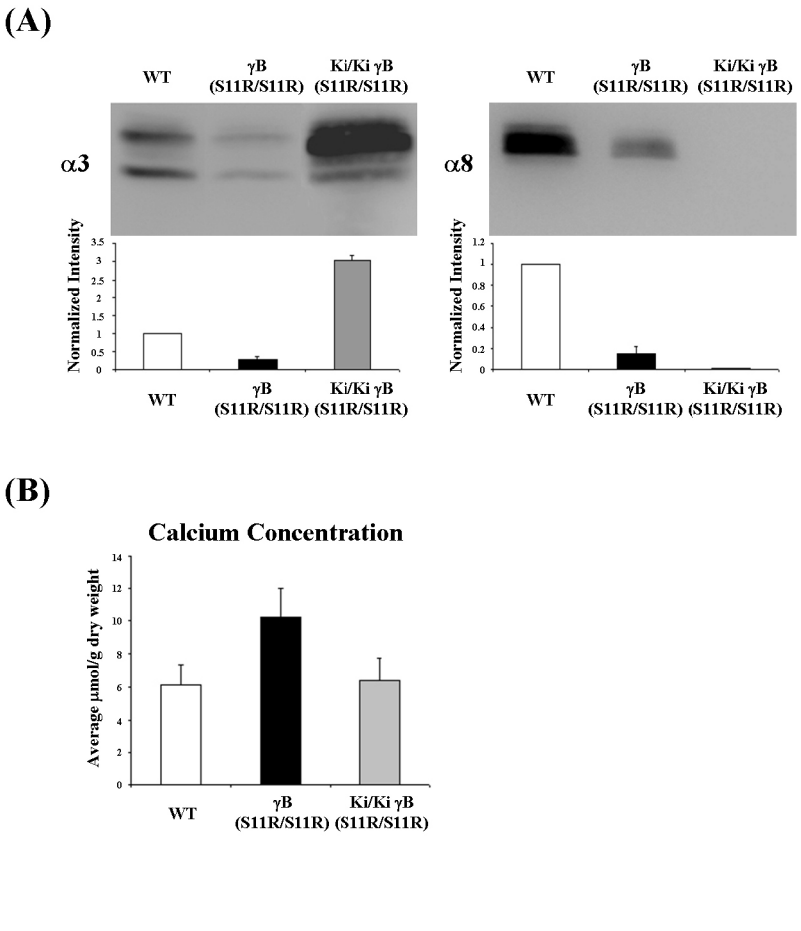
(A)
WT
γB (S11R/S11R)
Ki/Ki γB (S11R/S11R)
α3
α8
Normalized Intensity
(B)
Calcium Concentration
Average μmol/g dry weight
(C)
αA
αA-C1
αA-C2
αB
αB-C1
αB-C2
β
γ
Actin

Figure 9. Biochemistry studies of lens connexin, total calcium concentration and crystallin proteins of postnatal day 10 (P10) WT, γB(S11R/S11R) and Ki/Ki γB(S11R/S11R) lenses. (**A**) Representative Western blotting image of α3 connexin showed that there was about a 4-fold decrease in the γB(S11R/S11R), and about a 3-fold increase in the Ki/Ki γB(S11R/S11R) lenses compared to WT lenses. There was also a 5-fold decrease of α8 connexin in the γB(S11R/S11R) and no α8 was detected in the Ki/Ki γB(S11R/S11R) lenses. (N=3, $P<0.05$) (**B**) Total amount of calcium in the lens was measured by ICP-OES. In comparison to WT lenses, calcium concentration was increased in γB(S11R/S11R) lenses; total calcium level was back to the WT level in Ki/Ki γB(S11R/S11R) lenses. All the differences were statistically significant. (N=4, $P<0.05$) (**C**) Cleaved αA-, αB-, β- and γ-crystallins were detected in P10 γB(S11R/S11R) mutant lenses (arrowheads). There were two major αA- and αB-crystallin degradation products (αA-C1, αA-C2 and αB-C1, αB-C2) in the γB(S11R/S11R) lenses. However, only cleaved form γ-crystallins and very little of αB-C1 were detected in P10 Ki/Ki γB(S11R/S11R) rescue lenses with no other crystallin cleavage as WT. Total amount of β–actin remained unchanged between different lenses.

3.4.3 Normal Distribution of F-actin and Cytosolic Gamma-crystallin in Inner Fiber Cells

We carried out γ-crystallins immunostainning with double labeling of F-actin for P1 wild-type, γB(S11R/S11R) and Ki/Ki γB(S11R/S11R) lenses. γB-S11R mutation caused abnormal membrane-associated γ-crystallins aggregation and abolished actin filament in mature fiber cells as previously reported (Li et al., 2008). We believe that was upstream of fiber cell degeneration and protein degradation. However, in Ki/Ki γB(S11R/S11R) lens, γ-crystallins became more uniformly distributed with weak membrane-associated signal. F-actin was preserved in the position where we had seen F-actin disruption in γB(S11R/S11R) sample (Figure 10A). We also evaluated the distribution of α3 connexin. Because of the degeneration of inner fiber cells, α3-connexin signal was disrupted and F-actin disassembled in the middle fiber cells. The α3-connexin signal in the Ki/Ki γB(S11R/S11R) lens displayed a stronger and regularly punctuate signal as compared to the wild-type (Figure 10B).

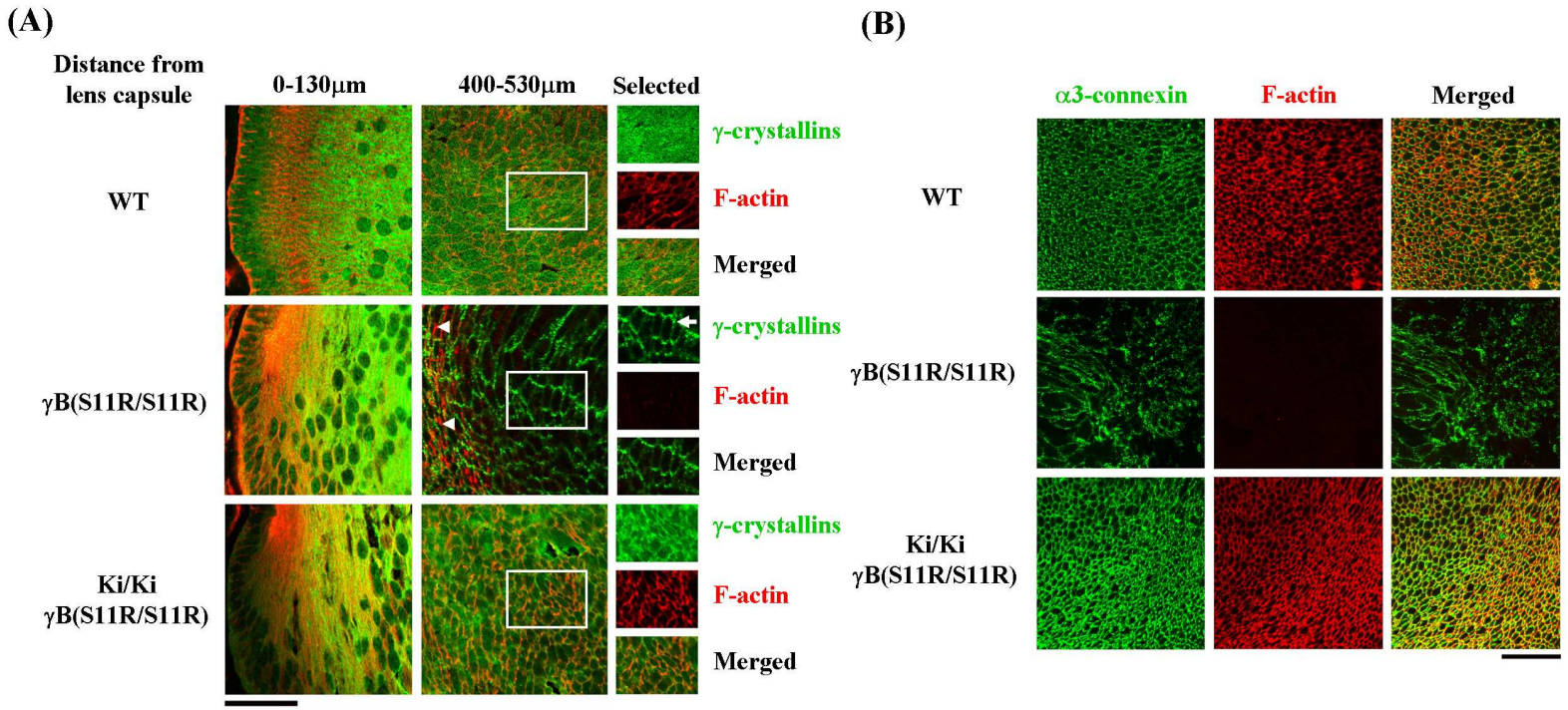
(A)
Distance from lens capsule
0-130μm
400-530μm
Selected
WT
γB(S11R/S11R)
Ki/Ki γB(S11R/S11R)
γ-crystallins
F-actin
Merged
(B)
α3-connexin
F-actin
Merged
WT
γB(S11R/S11R)
Ki/Ki γB(S11R/S11R)

Figure 10. Immunostaining of γ-crystallins and α3-connexin with actin filaments in lens fiber cells. (**A**) Postnatal day 1 (P1) WT, γB(S11R/S11R) and Ki/Ki γB(S11R/S11R) lens frozen sections were stained with anti-γ-crystallin antibody (*green*) and rhodamine-phalloidin (*red*). Boxes represent selected areas that show separated and merged fluorescent images of γ-crystallin and F-actin in lens inner fiber cells. White arrows indicate γ-crystallin aggregates adjacent to cell boundaries, white arrowheads indicate F-actin aggregation and disassembly. There was no F-actin in the most inner fiber cell (460-530μm from lens capsule). The γ-crystallins in the Ki/Ki γB(S11R/S11R) lens remained cytosolic and actin filaments sustained in inner fiber cells. Scale bars, 50μm. (**B**) Immunostaining of α3-connexin and actin filaments in inner fiber cells. Postnatal day 7 (P7) WT, γB(S11R/S11R) and Ki/Ki γB(S11R/S11R) lens frozen sections were stained with anti α3-connexin antibody (*green*) and rhodamine-phalloidin (*red*). Separated and merged fluorescent images are shown. Of note is that α3-connexin signal was disrupted due to degeneration of inner fiber cells, and F-actin disassembled in inner fiber cells. The α3-connexin in the Ki/Ki γB(S11R/S11R) lens displayed a stronger and punctuate signal as compared to the WT. Scale bars, 50μm.

3.4.4 Histology Reveals Normal Inner Fiber Cells in Knock-in Mutant Lenses

Cytoskeletal structure disruption in γB(S11R/S11R) lens lead to disorganization of fiber cell packing and degeneration of inner fiber cell (Figure 11 middle panel). Enlarged extracellular spaces were seen between 500-580μm region from the lens cortex (*arrowheads*). Disintegrated inner fiber cells were loosely attached (*arrows*). Since F-actin was maintained in Ki/Ki γB(S11R/S11R) lens so that fiber cell remained normal morphology in the same region of interest. Tightly packed inner fiber cells were seen similar to those in the wild type. However, abnormal Toluidine blue-stained intracelluar aggregates were found in Ki/Ki γB(S11R/S11R) lens as also seen in γB(S11R/S11R). Those aggregates did not abolish the fiber cell packing and were probably caused by γB-S11R mutation itself. Molecular mechanism of these aggregates needs further investigation.

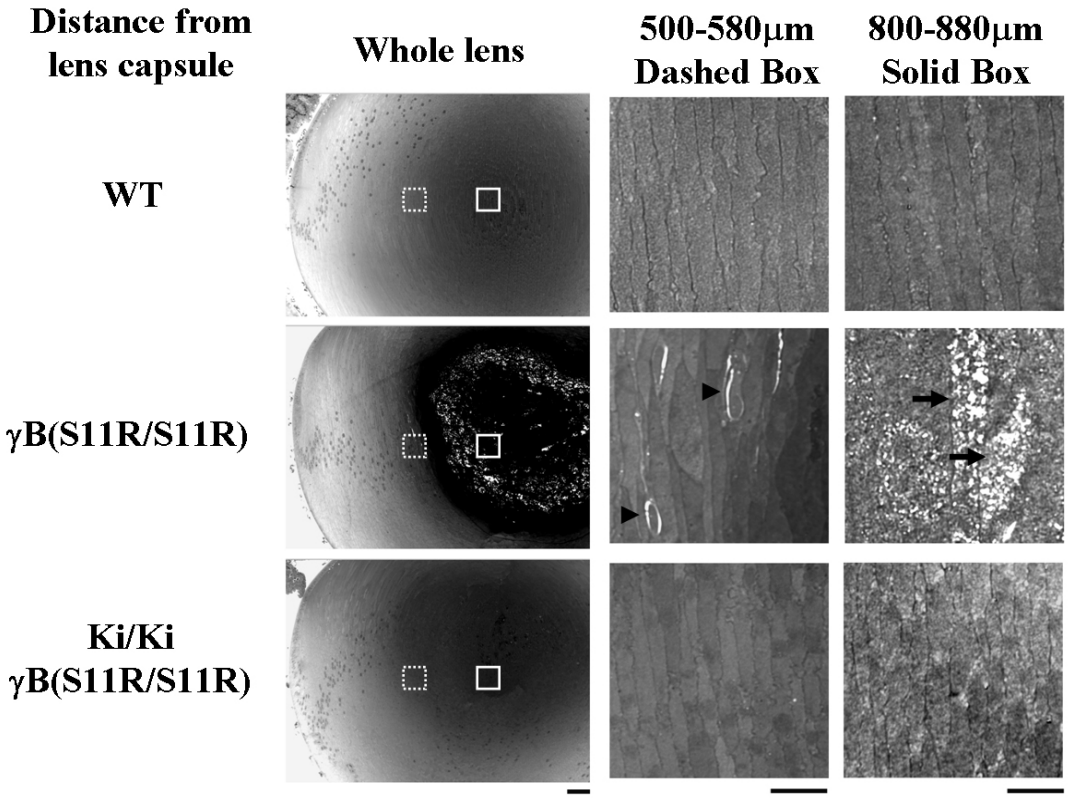

Figure 11. Histology of P7 WT, γB(S11R/S11R) and Ki/Ki γB(S11R/S11R) mutant lenses. Whole lens sections are shown on the left column. Scale bar, 100μm. High magnification images of selected area are shown in the middle column (*dashed square*) and right column (*solid square*). The transitional region of differentiating and mature fiber cell in γB(S11R/S11R) lenses (500-580μm from lens capsule) displayed enlarged extracellular spaces (*arrowheads*), and only γB(S11R/S11R) lenses revealed disintegrated fiber cells (*arrow*) in the nuclear region of the lens (800-880μm from lens capsule). WT and Ki/Ki γB(S11R/S11R) lenses showed elongated and tightly packed fiber cells. Scale bars, 20μm.

3.4.5 Dosage Effect of One Allele Knock-in α3 Connexin Partially Rescue Model

We have shown above that two α3 connexin knock-in alleles can rescue the nuclear cataract caused by γB-S11R mutation. We evaluated whether one knock-in allele versus two could have differences on cataract suppression. Ki/- α3(-/-) γB(S11R/S11R) and Ki/Ki α3(-/-) γB(S11R/S11R) were generated from several generation intercrossings of Ki/Ki γB(S11R/S11R) and α8(-/-) α3(-/-) double knockout (DKO). To our surprise, Mutant mice containing only one knock-in allele displayed various phenotypes at about one month old. Some Ki/- α3(-/-) γB(S11R/S11R) lenses were clear of nuclear cataract as Ki/Ki α3(-/-) γB(S11R/S11R); while some lenses showed relatively severe and intermediate nuclear cataracts (Figure 12). Two allele knock-in samples were completely rescued without individual variation.

We tested the biochemical difference between 1M α8(Ki/-) α3(-/-) γB(S11R/S11R) different phenotype samples. Western blotting of crystallin proteins revealed that there were more cleaved αA-, αB-, β- and γ-crystallins in 1M α8(Ki/-) α3(-/-) γB(S11R/S11R) severe and intermediate samples than mild samples (Figure 13, *arrowheads*). No cleaved crystallin was detected in WT lenses, and only αB-C1 and γ-C2 were detected in α8(Ki/Ki) α3(-/-) γB(S11R/S11R) lenses (data not shown).

We traced back when the phenotype had no difference, whether we had already detected any biochemical change. Lenses from a whole litter of P12 and P18 Ki/- -/- γB (S11R/S11R) mice were imaged and lens total protein was prepared. Lens phenotypes of postnatal day 12 old (P12) Ki/- -/- γB(S11R/S11R) and postnatal day 18 old (P18) Ki/- -/- γB(S11R/S11R) lenses showed no nuclear cataract (Figure 14A and B, *top*). Western blotting of α3 connexin, αA- and αB-crystallins of same lenses indicated that α3 connexin is unchanged between samples. However, one of the lenses (lens 1) had increased amount of cleaved both αA- and αB-crystallins than others. Some lenses were free of certain cleavage bands. The same trend was observed in postnatal day 18 (P18) Ki/- -/- γB(S11R/S11R) lenses (Figure 14A and B). It clearly showed that at the molecular level, even lens phenotypes were the same, and the cleaved protein product amount had differences. It is possible that those P12 and P18 lenses with more protein degradation will lead to more severe phenotypes, and vice versa.

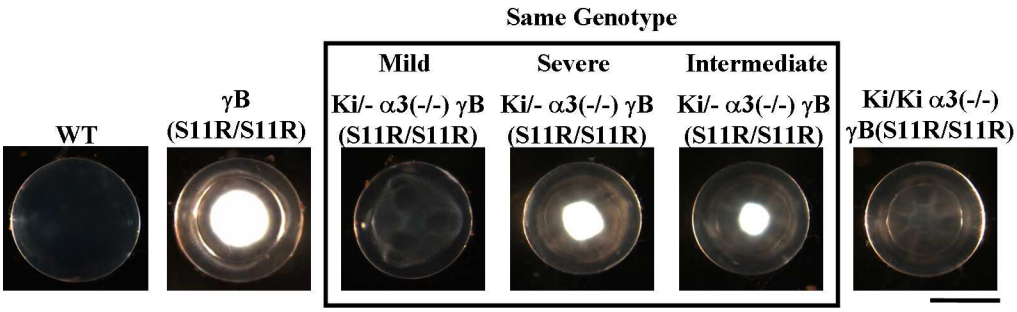

Figure 12. Lens pictures of one allele knock-in α3 connexin. Lens pictures of WT, γB(S11R/S11R), three α8(Ki/-) α3(-/-) γB(S11R/S11R) and α8(Ki/-) α3(-/-) γB(S11R/S11R) at the age of one month old (1M). Of note is that one allele Ki (symbol as α8(Ki/-) α3(-/-) γB(S11R/S11R)) created various phenotypes (mild, severe and intermediate) while two allele knock-in α8(Ki/Ki) α3(-/-) γB(S11R/S11R) only showed rescue phenotype. Scale bar, 1mm.

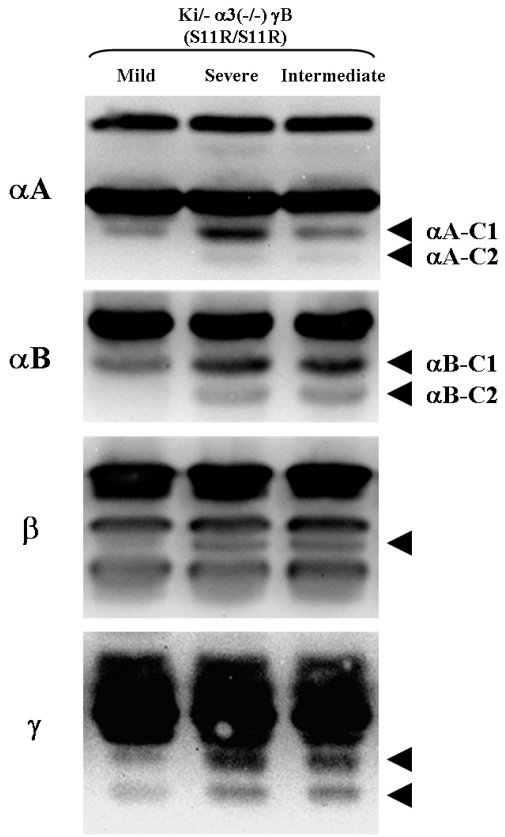

Figure 13. Representative Western blotting image of 1M α8(Ki/-) α3(-/-) γB(S11R/S11R) different phenotype samples. Western blotting of crystallin proteins revealed that there were more cleaved αA-, αB-, β- and γ-crystallins in 1M α8(Ki/-) α3(-/-) γB(S11R/S11R) severe and intermediate samples than mild samples (*arrowheads*).

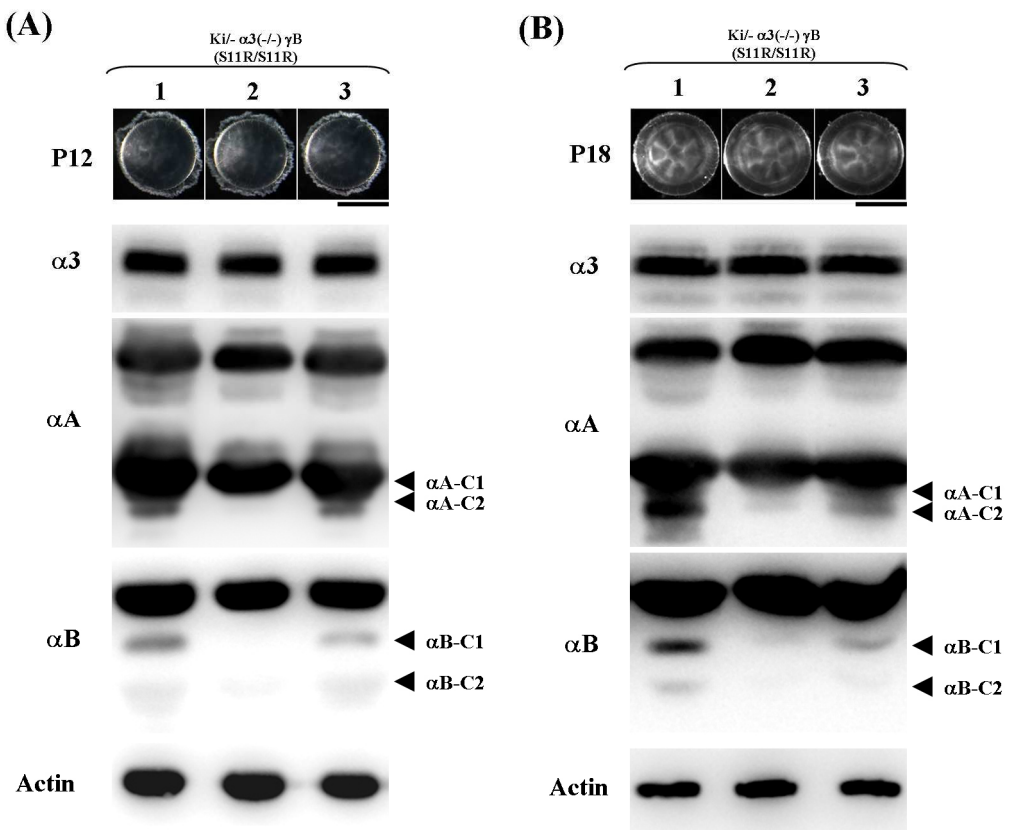

Figure 14. Lens picture and biochemistry studies of younger Ki/- -/- γB(S11R/S11R) lenses before phenotypes develop. (**A**) Representative lens picture of postnatal day 12 (P12) Ki/- -/- γB(S11R/S11R) lenses and Western blotting image of α3 connexin, αA- and αB-crystallins of all three lenses (1, 2 and 3). The lens is free of nuclear cataracts at P12. α3 connexin is unchanged between samples. However, lens 1 had increased cleaved αA-C1, αA-C2, αB-C1 and αB-C2 than lens 3. Lens 2 was free of αA-C1, αA-C2 and αB-C1, αB-C2. Total amount of β–actin remained unchanged between different lenses. (**B**) Representative lens picture of postnatal day 18 (P18) Ki/- -/- γB(S11R/S11R) lenses and Western blotting image of α3 connexin, αA- and αB-crystallins of all three lenses (1, 2 and 3). The lens is free of nuclear cataracts at P18. α3 connexin is unchanged between samples. However, lens 1 had increased cleaved αA-C1, αA-C2, αB-C1 and αB-C2 than lens 3. Lens 2 was free of αA-C1 and αB-C2. Total amount of β–actin remained unchanged between different lenses.

3.5 Discussion

3.5.1 Summary

We have genetically tested the feasibility for preventing a dense nuclear cataract caused by γB-crystallin-S11R mutation by using α3 connexin knockin mice, α3 connexin gene replacing endogenous α8 connexin gene. Remarkably, one allele of knockin α3 delayed the formation of the nuclear cataract and two knockin alleles completely prevented this dense nuclear cataract. Both morphological and biochemical data confirm that cataract prevention was correlated with the preservation of actin filaments and fiber cell integrity, as well as the inhibition of calcium elevation and crystallin degradation. Thus, knockin α3 connexin rescues the nuclear cataract by suppressing pathological processes caused by a γB-crystallin-S11R mutant protein *in vivo*. Although this is the first case that a crystallin mutation can be rescued by knock-in α3 connexin, we believe that this mechanism also applies to other crystallin point mutation caused cataracts. Preliminary unpublished data have shown that knock-in α3 connexin can rescue lens posterior rupture caused by γD-crystallin-V76D (Wang et al., 2007b) and improve lens clarity for *L10* mice caused by γB-crystallin-I4F mutation (Liu et al., 2005).

3.5.2 Implications of Experimental Results

Previous studies have shown that the knocked-in α3 subunits behave differently from the endogenous α3 subunits: 1) knocked-in α3 subunits are expressed under the α8 promoter, knocked-in α3 subunits are found in lens epithelium and expressed earlier than the endogenous α3 subunits (Martinez-Wittinghan et al., 2003); 2) the protein level of knocked-in α3 is higher than that of endogenous α3 (shown in Figure 9A); and 3) knocked-in α3 subunits form pH-sensitive gap junction channels between differentiating fibers (Martinez-Wittinghan et al., 2004). We have observed a significant decrease of α3 and α8 connexin levels in γB(S11R/S11R) lenses, thus knock-in α3 connexin can compensate the loss of connexins. Abnormal γ-crystallin aggregates and F-actin loss are found in new-born γB(S11R/S11R) lenses when calcium concentrations have risen to a critical level to activate calpains on P7. Histology data indicate that fiber cells have already severely degenerated by P7. Earlier and stronger α3 connexin expression may 1) facilitate calcium transport out from fiber cells in embryonic stage so that calcium cannot accumulate; 2) facilitate special signal transductions that can prevent γ-crystallin aggregation and F-actin loss; and 3) enhance cell-cell adhesion and integrity.

In the knockin lenses, the coupling conductance of mature fibers is about doubled compared to the wild-type, and calcium concentration in the center drops by about 30% (Gao et al., 2004). Previous findings have also shown that α3 connexin is responsible for the coupling in mature fiber cells while α8 connexin functions mainly in the differentiating fibers (Baldo et al., 2001; Gong et al., 1998). When α8 is replaced by α3 connexin, gap junctions channels originally formed by α8 connexins now all become α3 connexin channels, with higher expression levels. This can explain why the coupling conductance doubles and calcium concentration decreases in the knock-in lens. However, signals that control proper lens growth seem to only go through α8 connexin channels, and even with α3 connexin present at the same location where α8 connexin ought to be, a small lens defect is not rescued. The lens size is correlated with the epithelial cell proliferation rate which is influenced by α8 connexin (Sellitto et al., 2004; White et al., 2007; White et al., 1998), but knock-in α3 connexin could not restore central and equatorial epithelial proliferation (White et al., 2007). This suggests that α8 connexin selectively mediates the passage of certain second messengers of growth factor signal transduction, resulting in a proper cell mitotic rate, particularly in the central epithelium (White et al., 2007).

Thus far, factors causing membrane-associated γ-crystallin aggregation and F-actin disassembly in γB-S11R mutant lens are unknown. When transfecting γB-S11R mutant protein in immortalized human lens epithelial cell line, γB-S11R looks the same as wild-type protein without membrane-associated γ-crystallin aggregation under normal culture conditions (data not shown). This suggests that some additional factors are present only in mature fiber cells of lens nucleus triggering γ-crystallin aggregation adjacent to the cell boundary and disruption of cytoskeleton structure in γB-S11R mutant lens. In knock-in and γB-S11R compound mutant lenses, γ-crystallins remain mostly in cytosol and F-actin is preserved in the newborn stage. However, there are still membrane-associated γ-crystallins in newborns and F-actin loss at P21.

We speculate that those unknown factors still exist, but do not accumulate as quickly as in the γB-S11R mutant lens, giving the fact that knock-in α3 can facilitate chemical and signal transductions. There is no direct evidence that α3 or α8 connexins interact with cytoskeletal proteins such as actin. However, studies have shown that cytoskeletal proteins, especially actin, are crucial for connexin anchorage to the cell membrane and to the formation of gap junctions (Giepmans, 2004; Qu et al., 2009). It is possible that knock-in α3 recruits actin around the plasma membrane and helps maintain F-actin structure.

As gap junction formation requires proper adhesive cell-cell interactions, there must be a relationship between gap junctions and adhesion molecules/adherens junctions. In cultured embryonic lens cells, gap junction formation is inhibited by antibodies to N-cadherin (Frenzel and Johnson, 1996). Antibodies against E-cadherin and N-cadherin can alter the formation of gap junctions (Jongen et al., 1991; Meyer et al., 1992), and likewise, antibodies against α1 connexin (Cx43) can inhibit the assembly of adherens junctions (Meyer et al., 1992). In addition, α1 connexin and N-Cadherin form a multiprotein complex in NIH3T3 cells; siRNA knock-down of α1 connexin causes decreased expression and membrane localization of N-cadherin and N-cadherin-associated proteins (Wei et al., 2005). A new study also suggests that connexin hemichannels can establish adhesive interactions between cells independently of forming functional gap junctions (Cotrina et al., 2008). Given above evidence, it is reasonable to hypothesize that knock-in a3 connexin can enhance cell-cell adhesion. Lens transparency and high refractive index rely on the tight packing of fiber cells. Enlarged extracellular spaces in γB-S11R mutant lens are probably due to the loss of adhesive contact between fibers. In contrast, compound mutant lenses display organized and tightly packed fibers, suggesting that an overexpression of α3 connexin would contribute to the enhancement of cell-cell adhesion.

3.5.3 Dosage Effect of Knock-in α3 Connexin

It is intriguing to learn that one allele knock-in α3 connexin only partially rescues or delays the onset of nuclear cataract caused by γB-S11R mutation; it is also interesting that there are huge phenotypic variations between mice of the same genotype, sometimes even between left and right lenses of the same mouse. At P18, most of lenses contain one allele knock-in show clear lens, however, a few days later, we can observe various lens phenotypes. Rapid progression of cataract severity suggests that something may already be changed before we can see the phenotype. These mice share the same genotype, meaning that gene expression should be identical. Western blotting data confirms that α3 connexin levels remain unchanged between samples. However, we find that αA- and αB-crystallin cleavage patterns are different in young Ki/- -/- γB(S11R/S11R) littermate lenses before phenotype differentiates. This guides us to correlate the amount of αA- and αB-crystallin cleavages and cataract severities. We predict that the clear or mildly cataractous mutant lenses should have no obviously or slightly increased αA- and αB-crystallin cleavages at P12 and P18. Beta-crystallin and γ-crystallin cleavages are different at 1M but not at P12 and P18 (data not shown), suggesting β-crystallin and γ-crystallin are less sensitive to the calpain activation. AlphaA- and αB-crystallins may be good markers for pathological event caused by calcium-dependent protein degradation. These biochemical differences indicate why and how one allele knock-in α3 connexin influences the lens phenotypes.

Chapter 4 Studies of Genetic Suppressor for Nuclear Cataracts

4.1 Preface of Chapter

The purpose of this part of my thesis project is to identify the genetic modifier(s) in C57BL/6J strain background that suppresses a nuclear cataract caused by a loss of α3 connnexin (Gja3 or Cx46) and to investigate the molecular mechanism for the regulation of nuclear cataract formation.

A genome-wide linkage analysis was performed on α3 knockout mice generated from both intercross and backcross between C57BL/6J (B6) strain background and 129SvJae (129) strain background. Nuclear cataracts of living animals were evaluated by slit lamp examination. The degree of nuclear opacity was quantified by measuring light scattering with a fiber optic spectrometer. Western blotting was used to determine the biochemical changes associated with variable nuclear cataracts.

The lod scores of genome-wide linkage analysis indicated genetic modifiers may be located on chromosome 2 (D2Mit148), chromosome 7 (D7Mit230) and chromosome 9 (D9Mit11). Backcrossed α3 knockout mice (B6 α3 knockout mice backcrossing into the 129 strain background) containing D7Mit294 locus of B6 strain displayed an intermediate degree of nuclear cataracts. Intercrossed α3 knockout mice with two alleles D7Mit294 of B6 strain developed mild nuclear cataracts similar to mutant mice in the B6 background while intercrossed α3 knockout mice with two alleles D7Mit294 of 129 strain displayed severe nuclear cataracts. Western blotting results showed that the severity of nuclear cataract was associated with the amount of cleaved crystallins.

We have mapped a dominant suppressor of nuclear cataracts which is located on chromosome 7 of B6 strain background near genetic marker D7Mit294. The severity of nuclear cataracts is correlated to the amount of cleaved forms of crystallin proteins in α3 knockout lenses. This genetic suppressor probably functions at the upstream of the regulation of calcium homeostasis and/or the activation of the calpain proteases, which are responsible for cleaving crystallin proteins in the lens. Fine mapping and candidate gene characterization will lead to the identification of this genetic modifier that prevents nuclear cataract formation.

4.2 Introduction

Previous studies have reported that dense nuclear cataracts in the 129SvJae (129) α3 knockout mice likely resulted from the cleavages of crystallin protein, especially γ-crystallin (Gong et al., 1997). However, C57BL/6J (B6) α3 knockout mice only showed mild nuclear cataracts with minimal crystallin degradation, suggesting there was a genetic suppressor(s) in B6 mouse strain suppressing severe nuclear cataract development. γ-crystallin cleavage was absent in the B6 α3 knockout lenses. Mix background α3 knockout mice of 129 x B6 strains developed various cataract phenotypes and severities of cataract were correlated with the crystallin degradations. The mild phenotype lenses had less γ- and αB-crystallin degradations than severe lenses (Gong et al., 1999).

The proteolysis of crystallins is correlated with lens calcium accumulation that is resulted from the lack of gap junction channels formed by α3 connexin. Thus, calcium elevation would activate calcium-dependent proteases in the cell such as calpains that cleave crystallins. Recently, calpain3,Lp82/Lp85 isoforms, is verified to be an essential protease for the unique degradation of γ-crystallin, 11kD cleaved gamma crystallin, in the α3 knockout lens (Tang et al., 2007). Double knockout of calpain 3 and α3 connexin displayed very mild cataract in the 129 strain background. However, it remains unclear whether or not calpain3 directly cleaves γ-crystallin

Genetic suppressors on the Chr7 and on another chromosome of the B6 strain background remain to be identified. Previous studies via genetic and proteomic approaches have elucidated substantial information about the downstream effects of these genetic modifiers in cataractogenesis associated with a lack of α3 connxin in the lens (Gong et al., 1999; Hoehenwarter et al., 2008; Tang et al., 2007). This part of my thesis has further mapped one specific genetic modifier to an approximate region to the linkage marker D7Mit294 on Chr 7. We hypothesize that this genetic suppressor reduces the nuclear cataract by inhibiting the proteolysis of crystallin proteins via the prevention of calpain activation or calcium elevation in the lens.

4.3 Methodology and Materials

4.3.1 Animals

Mouse care and breeding were performed according to the Animal Care and Use Committee (ACUC)-approved animal protocol (UC Berkeley) and the ARVO Statement for the Use of Animals in Ophthalmic and Vision Research. Mouse pupils were dilated with 1% atropine and 1% phenylephrine before the eyes were examined for lens clarity by a slit lamp.

G0 129SvJae and G0 C57BL/6J α3 knockout mice were crossed to generate G1 129/SvJae x C57BL/6J hybrid α3 knockout mice. G1 mice were intercrossed to generate F2 hybrid mice for genome-wide genetic linkage analysis. G1 mice were backcrossed to 129/SvJae α3 knockout mice to generate G2 hybrid mice. The G2 mouse with mildest phenotype was screened by slit lamp examination and backcrossed again to 129/SvJae α3 knockout mice to generate G3 mice and so on. Mice with one selective C57BL/6J allele of D7Mit294 locus (D7Mit294 (129/B6)) were intercrossed to generate intercrossed 129/SvJae x C57BL/6J hybrid α3 knockout mice. Following three genotypes were generated: D7Mit294 (129/129), D7Mit294 (129/B6) and D7Mit294 (B6/B6).

4.3.2 Mouse Genotyping

A small piece of mouse tail was collected according to the animal protocol. Lysis buffer (100 mM Tris pH 8.0, 5 mM EDTA, 0.2% SDS and 200 mM NaCl) with proteinase K was added to dissolve the tail by shaking at 55^0C. Equal amount of isopropanol was used to precipitate DNA. DNA pellet was rinsed with 70% ethanol and dissolved in TE buffer (10 mM Tris-Cl pH 7.5 and 1 mM EDTA). A standard PCR method was used to genotype different satellite markers. Genetic marker sequences are listed in table 2.

Marker Name	**Left Primer Sequence**	**Right Primer Sequence**
D7Mit154	CTGTAGAAAATTAAGATGTTGGATTTG	CTGGCTCTATCAGAAATATATGGTG
D7Mit23	CTGGCTGCACCAGTGATG	ACTCTCAGCCAAATTTGAAAGC
D7Mit115	GCTTCGGTGTCTCTCTCTTTC	ACTGAGGGTCCATGACTTGTG
D7Mit144	AGACACTCATATGGTGCAGGG	GAGATTAAAGGTTTGTGCTGCC
D7Mit294	**TAGTGGGAAAGAGAGAAACAATCC**	**TAATGTTTAATCTTGTCGTCTTAGTGG**
D7Mit266	TCAGGGATGTCTTAAAACTGGG	CGCTGTAAAGCGTATTCGTG
D7Mit117	GCAATAGTTTTTCAGGGAGGG	CTATCTAAGAAAGTTGGACTGCAGC
D7Mit155	GTTGGAGAAATGACACCATGG	ACTTTACACACTGATCACTTTTCAGC
D7Mit230	GGGTTAACTGCTTTTTAAAAGTGC	ACTTCTGCATGTTGCCCTCT
D2Mit148	GTTCTCTGTCTACGGGCATG	TTCACTTCTACAAGTTCTACAAGTTCC
D9Mit11	GCCTTCATGTGTACCTGAATGCAC	GGCTCTGTAATCACTGAAGCTGT

Table 2. Genetic marker sequences for fine mapping.

4.3.3 Western Blotting

Lens total proteins were prepared by homogenizing enucleated fresh lenses that were weighed and homogenized directly in the sample buffer (60 mM Tris, pH 6.8, 2% SDS, 10% glycerol, 5% β-mercaptoethanol, and 0.001% bromophenol blue). To prepare the water insoluble protein samples, two frozen lenses were homogenized in 0.1 M NaCl and 50 mM Na_2HPO_4 (pH 7) at 40 mg lens wet weight/ml solution. The insoluble material was collected after centrifugation at 15,000 rpm for 15 min and washed once with the same solution. This insoluble pellet was dissolved in the sample buffer. Equal volumes of samples were loaded on a 12.5% SDS-PAGE gel for separation, and separated proteins were transferred to a polyvinylidene difluoride membrane (Bio-Rad, Hercules, CA). Lens crystallin proteins were detected by Western blotting with rabbit polyclonal antibodies against αA-, αB- and γ-crystallins (generously provided by Joseph Horwitz at the University of California, Los Angeles), β-crystallin (generously provided by J. Samuel Zigler at the National Eye Institute), and a mouse monoclonal antibody against β-actin (Sigma, St. Louis, MO). More than three sets of lens protein samples of different mice were examined, and representative data were shown.

4.3.4 Fresh Lens Imaging and Light Scattering Quantification

Mice were euthanized by CO2 asphyxiation according to the ACUC-approved animal protocol. Fresh lenses, dissected from enucleated eyeballs, were immediately immersed in PBS at 37°C. Fresh lenses were imaged under a Leica MZ16 dissecting scope using a digital camera. Light scattering in the lenses caused by cataract was measured using the HR 2000CG_UV_NIR High Resolution Spectrometer and a QP400-2-UV-VIS fiber optic cable (400 μm cable diameter) (Ocean Optics, Dunedin, FL). Lenses were illuminated by a white light source perpendicular to the equator of the lens. Scattered light was captured by the optic fiber with a whole acceptance of angle of 24.8°. Spectrums were recorded and saved for later comparison. Each lens was measured twice in succession to show repeatability. The measurements were represented as graphs with wavelength on the x-axis and light intensity on the y-axis. Denser cataracts scattered more light, and thus, the light scattering intensity measured by the detector increased. Measurements were stored as ASCII files, and area under the curve was calculated by a Matlab program.

4.4 Results

4.4.1 Dominant Nuclear Cataract Suppressors in C57BL/6J Mouse Strain

Alpha3 connexin knockout mice in 129/SvJ (129) background developed dense nuclear cataracts at 4-week-old, while in C57BL/6J background only displayed very mild nuclear cataracts (Figure 14A). G0 129 α3 knockout mice were crossed with G0 B6 α3 knockout mice to generate G1 129/B6 mix background α3 knockout mice. We have observed that all G1 mice displayed a mild lens phenotype suggesting genetic suppressor(s) had dominant effects (Figure 14A). G1 129/B6 hybrids were intercrossed to generate F2 α3 knockout mice. F2 mice produced varying degrees of nuclear opacity from the same litter, suggesting there were multiple factors (Figure 14B). Different genetic combinations of these multiple modifiers might lead to various lens phenotypes.

To further investigate the existence of genetic suppressors, G1 mice were backcrossed to 129 α3 knockout mice to generate G2 129/B6 hybrid mice. Lens phenotypes were examined by using a portable slit lamp, and various cataract severities were observed. Mouse with mildest cataract phenotype was picked and backcrossed to 129 α3 knockout mice to generate G3 129/B6 hybrid mice. G3 mice also displayed different cataract phenotypes varying from severe, intermediate to mild nuclear cataracts at 4-week-old, compared to a severe nuclear cataract in 129 and a mild nuclear cataract in B6 α3 knockout lenses (Figure 15A). Light scatterings by cataractous lenses were measured by the fiber optic spectrometer. 129 α3 knockout and G3 severe phenotype lenses showed dramatic light scattering indicated by the orange and red curves while G3 intermediate and mild lenses showed less intensity of light scattering in blue and green curves. B6 α3 knockout lenses only gave minimal amount of light scattering indicated by purple curve (Figure 15B). Areas under each curve were calculated by a MATLAB program and data was equivalent to what has been described above (Figure 15C). Differences between the three genotypes were statistically significant ($P<0.05$).

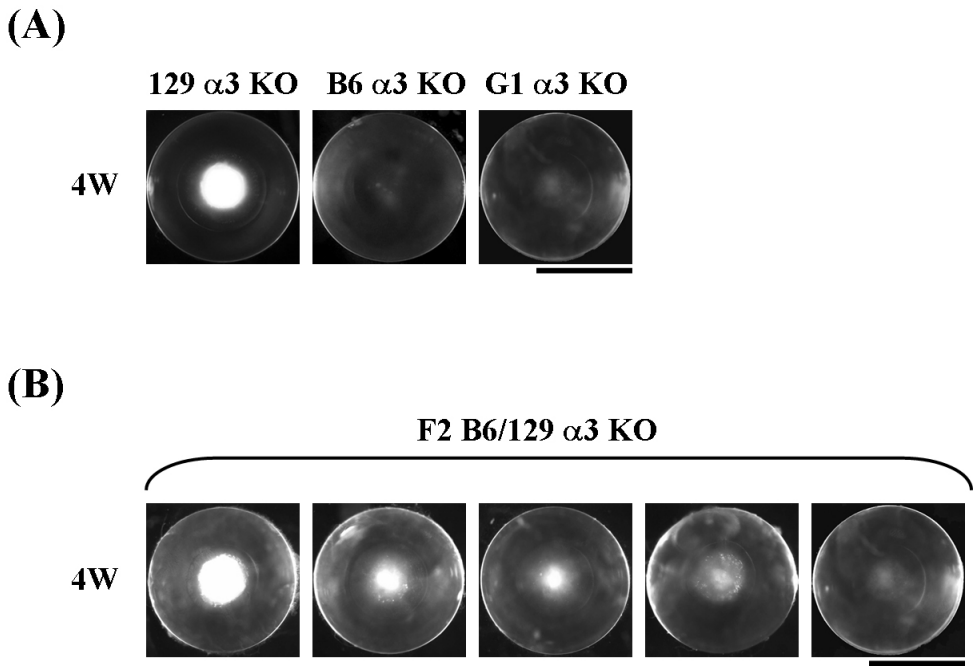

Figure 15. Dominant multiple suppressors in the C57BL/6J background. (**A**) A pure G0 129SvJae (129) α3 KO mouse with severe phenotype (left) and a G0 C57BL/6J (B6) α3 KO mouse with mild phenotype (middle) were crossed to create G1 α3 KO mice with all mild phenotype. This demonstrates the existence of dominant genetic modifier(s) in the B6 allele. Scale bar, 1mm. (**B**) The G1 129/B6 hybrid mice were intercrossed to obtain F2 129/B6 hybrid α3 KO mice that displayed various cataract phenotypes from severe, intermediate to mild (from left most to right most) suggesting there were multiple suppressors in the B6 genome. In order to determine the region where the genetic modifiers reside, mouse tails from F2 mice were collected for genome-wide linkage analysis. Scale bar, 1mm.

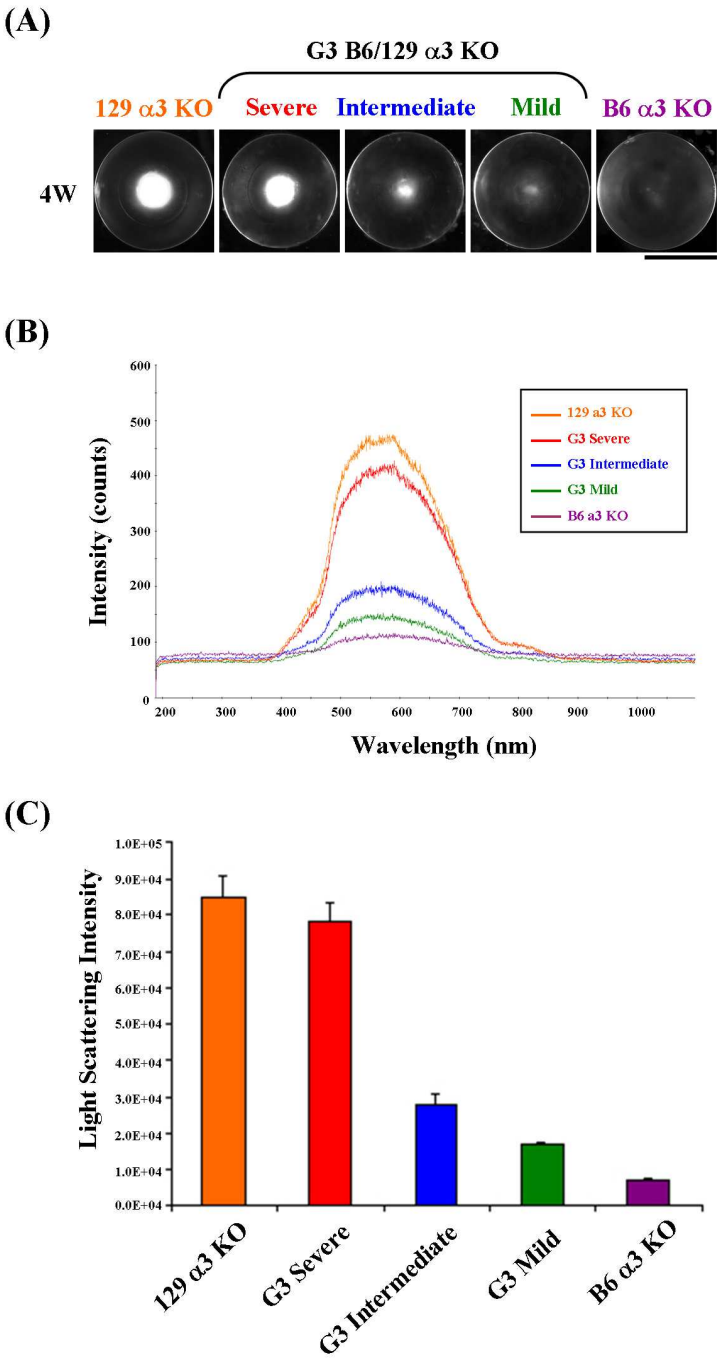
(A)
G3 B6/129 α3 KO
129 α3 KO
Severe
Intermediate
Mild
B6 α3 KO
4W
(B)
Intensity (counts)
Wavelength (nm)
129 a3 KO
G3 Severe
G3 Intermediate
G3 Mild
B6 a3 KO
(C)
Light Scattering Intensity
129 α3 KO
G3 Severe
G3 Intermediate
G3 Mild
B6 α3 KO

Figure 16. Backcrossed 129/B6 α3 KO mice showed various phenotypes. (**A**) Lens pictures of 4 weeks old (4W) G0 129 α3 KO, G3 backcrossed 129/B6 α3 KO hybrid and G0 B6 α3 KO mice. G0 129 α3 KO mice displayed severe nuclear cataracts (left). G3 backcrossed 129/B6 α3 KO hybrid mice showed severe, intermediate, and mild phenotypes (middle three pictures), and B6 α3 KO mice exhibited very mild nuclear cataracts (right). (**B**) Light scattering measurement of 4W 129 α3 KO, G3 Severe, G3 Intermediate, G3 mild, and B6 α3 KO lenses using optic fiber spectrometer. Each genotype is depicted according to the colors indicated. 129 α3 KO exhibited most dramatic light scattering while B6 α3 KO lenses displayed minimal amount of light scattering. (C) The areas under each curve were calculated and plotted in a bar graph. As previously indicated, 129 α3 KO had largest light scattering intensity and B6 α3 KO showed the least amount of scattering.

4.4.2 Genetic Suppressor(s) Is(Are) Linked to Chromosome 7 in C57BL/6J Mouse Strain

Genomic DNA collected from F2 α3 knockout mice was used to carry out genome-wide linkage analysis. Three genetic loci were shown linked to the genetic suppressor: D9Mit11, D7Mit230 and D2Mit148. All three loci had LOD scores that were above the 99% threshold (Table 3). Since there were multiple candidates, it was difficult to further keep track of which locus was really responsible for severe cataract suppression. We decided to test these three loci by using G3 and up mouse DNA.

We took the mild phenotype G2 mice backcrossed with original 129 α3 knockout mice again to generate G3 backcrossed mice and so on. The purpose is to generate mice mostly in 129 background but with selective alleles of the B6 strain. If offspring from many generations of backcrossing still showed mild to intermediate phenotype, then we know the suppressors are located in those selective B6 alleles and we would be able to identify the genes by fine mapping.

Genetic Locus	**LOD Score**
D9Mit11	5.72489184
D7Mit230	3.92550836
D2Mit148	2.97558673
99% Threshold	2.419066

Table 3. Lod scores of three candidate markers from initial genome-wide linkage testing

We collected DNA from G3 and up backcrossed α3 knockout mice, and carried out fine mapping using those three candidate markers from initial genome-wide screening. D9Mit11 and D2Mit148 seemed to have no correlation between genotype and phenotype. Subsequently, we identified that D7Mit230 showed strong correlation, where mice with two alleles D7Mit230 of the 129 strain showed severe phenotype and mice with one allele D7Mit230 of the B6 strain showed mild to intermediate lens phenotypes. This suggested that at least one of the genetic suppressors is located around the D7Mit230 locus.

After several generations of backcrossing, D7Mit230 no longer remained a good marker for genetic suppressor because “crossover” (genotype did not match phenotype) occurred before G9 generation. However, another two markers D7Mit294 and D7Mit144 showed no “crossover” thus far (Figure 16). D7Mit294 is a clear marker for distinguishing bands for 129 and B6 strain, however, bands for D7Mit144 are not very clear. D7Mit294 has become a good marker for the genetic suppressor on chromosome 7 unless “crossover” occurs at this locus.

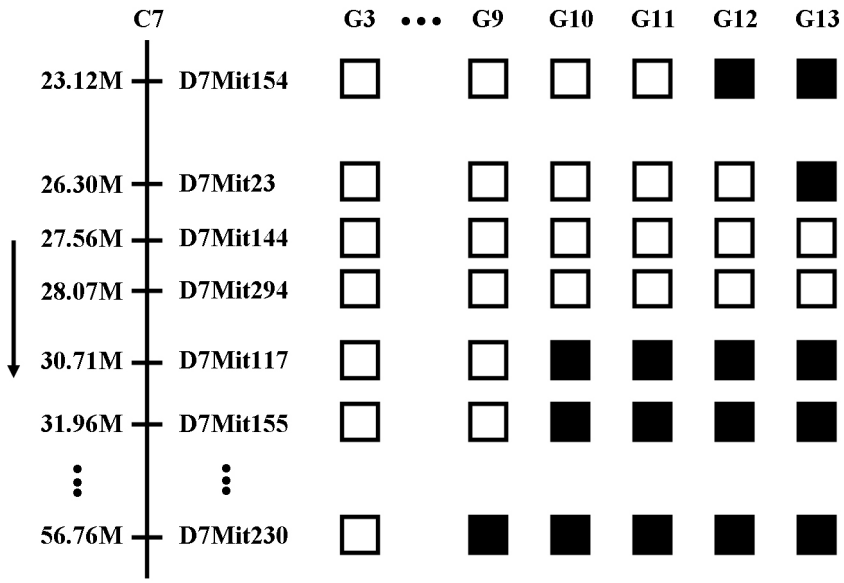

Figure 17. Fine mapping of the genetic suppressor on mouse chromosome 7. The genetic suppressor is mapped to a genetic locus near D7Mit230 with lod score of 3.925. Further fine mapping using satellite marker D7Mit294 with no crossover suggests that at least one of the modifiers may be located within this region of the chromosome. The solid black boxes indicate crossover events where the phenotype and genotype were mismatched, revealing the lack of genetic suppressor at that region. The outlined boxes are possible locations where the genetic modifier may reside, which are expected to be between 26.30 and 30.71 million base pairs region on chromosome 7.

4.4.3 Two Copies of D7Mit294 Allele of the B6 Strain Are Sufficient to Suppress Severe Cataract Formation in Mice Mostly in 129 Background

Since D7Mit294 was linked to the genetic suppressor(s), we want to investigate one copy of this locus verse two copies make a difference in cataract suppression. Mice with one selective B6 allele of D7Mit294 locus were intercrossed to generate offspring that might carry two 129 alleles, one 129 and one B6 allele or two B6 alleles of D7Mit294 locus. We want to evaluate whether two B6 alleles of D7Mit294 will further reduce the cataract phenotype. Figure 18A clearly shows that six-week-old (6W) mice with two B6 alleles of D7Mit294 (D7Mit294 B6/B6) displayed mildest phenotype and mice with one B6 allele (D7Mit294 129/B6) showed intermediate phenotype. Mice with two 129 alleles (D7Mit294 129/129) developed dense nuclear cataracts like 129 α3 knockout mice. Lens phenotypes were very similar at postnatal 18 days (P18), while two B6 alleles of D7Mit294 samples stayed relatively mild compared to one B6 allele and two 129 alleles at 3-week-old (3W). Cataract progression was clearly differentiated after 3W. Light scattering measurement shows that 6W D7Mit294 129/129 lenses displayed dramatic light scattering indicated by the red curve while 6W D7Mit294 129/B6 and 6W D7Mit294 B6/B6 lenses showed less light scattering indicated by blue and green curves (Figure 18B). We quantified the areas under each curve and plotted the bar graph. Differences between three genotypes were statistically significant (Figure 18C).

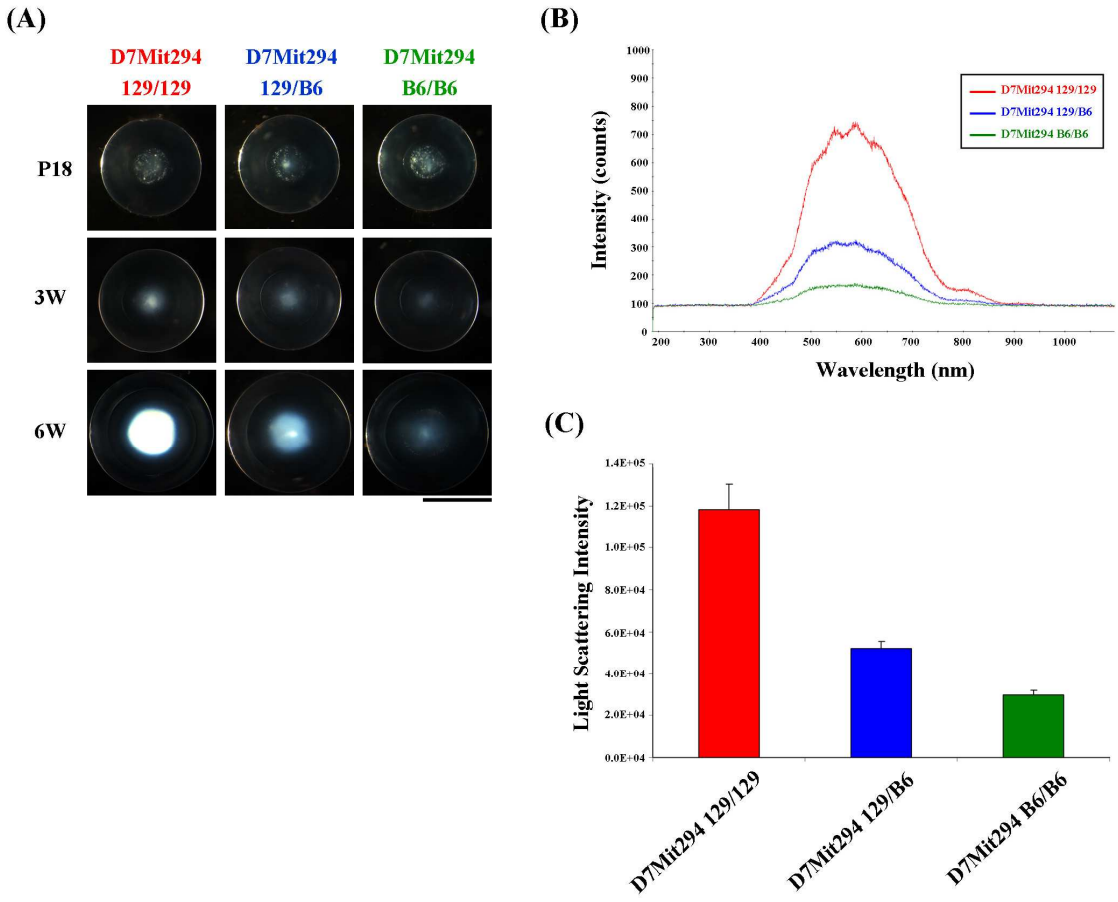

Figure 18. D7Mit294 is linked to the genetic suppressor(s). (**A**) Lens pictures of intercrossed D7Mit294 129/129, 129/B6, and B6/B6 at the age of postnatal 18 days old (P18), 3 weeks old (3W), and 6 weeks old (6W). At P18 and 3W, no major differences between the genotypes were observed. However at 6W, severe, intermediate, and mild phenotypes were easily distinguishable. (**B**) Light scattering measurement of D7Mit294 129/129, 129/B6, and B6/B6 using optic fiber spectrometer. Each genotype is depicted according to the colors indicated. D7Mit294 129/129 displayed the most dramatic light scattering while B6/B6 showed the least amount of light scattering. (**C**) The areas under each curve were calculated and plotted in a bar graph. As shown, D7Mit294 129/129 had the highest light scattering intensity and B6/B6 had the least.

4.4.4 Genetic Suppressor(s) Modulate(s) Crystallin Degradation

The original genetic modifiers in B6 strain modulate crystallin degradations. We want to evaluate whether the suppressor(s) on Chromosome 7 has similar effect. We purified insoluble proteins from 3-week-old (3W) and 6-week-old (6W) intercrossed samples and probed with different crystallin antibodies. Western blotting data on 6W revealed that D7Mit294 B6/B6 samples had less crystallin degradations compared to D7Mit294 129/B6 and D7Mit294 129/129 samples. On 3W, when no very obvious phenotype difference was seen on 3W, αB- and γ-crystallin already showed less cleavages in D7Mit294 B6/B6 samples compared to the other two (Figure 19A).

Lens total proteins of different ages were purified and Western Blottings of αB-crystallin were carried out. αB-C2 band was first noticed in new-born (P0) 129 α3 knockout and D7Mit294 129/129 samples. αB-C1 band was first noticed on postnatal 12 days (P12). αB-C1 and C2 band were significantly lighter in 3W D7Mit294 B6/B6 and B6 α3 knockout samples. On 6W, B6 α3 knockout had least αB-crystallin cleavages, while D7Mit294 B6/B6 samples had less αB-crystallin cleavages than the rest three samples (Figure 19B).

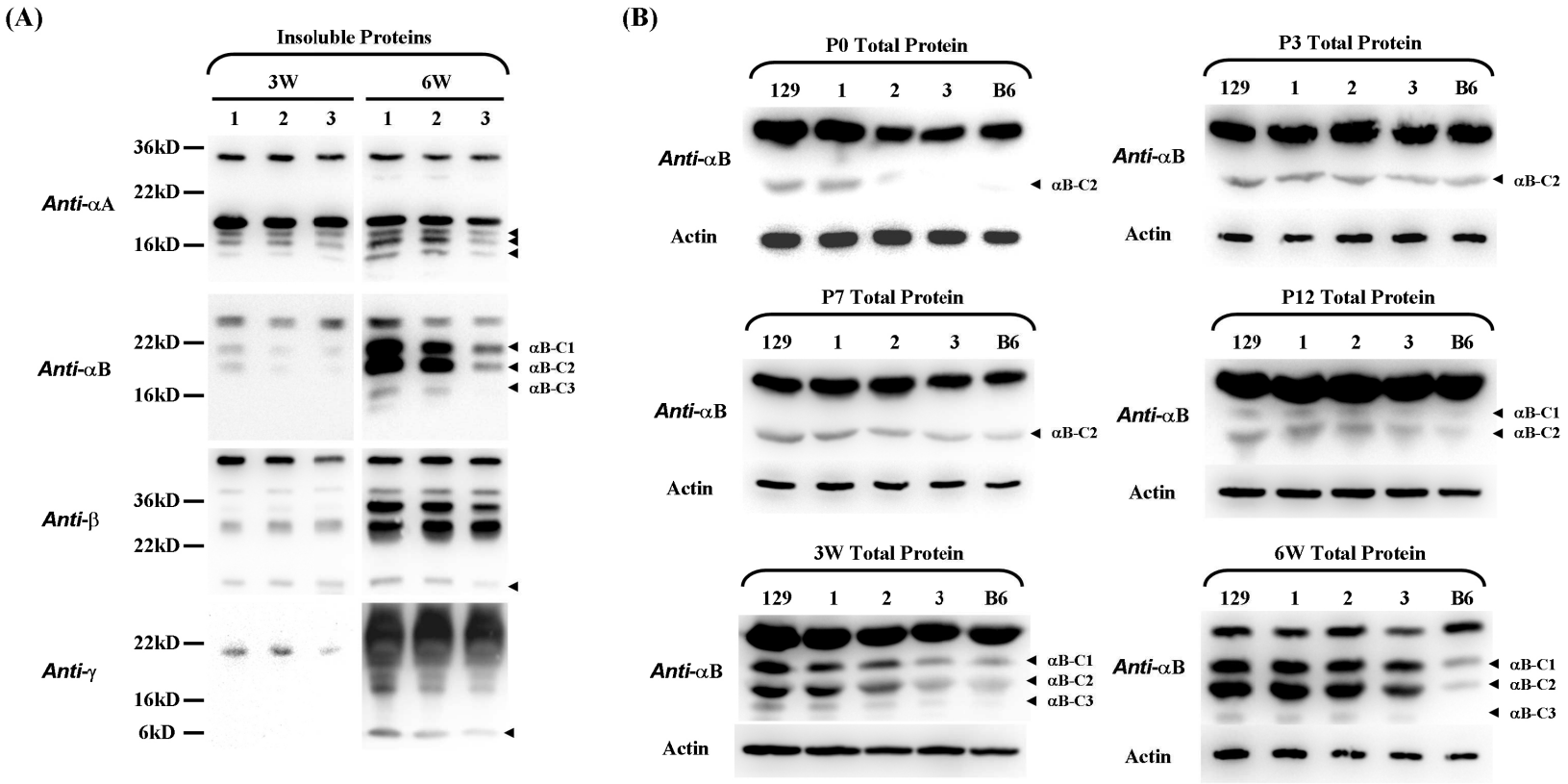
(A)
Insoluble Proteins
3W
6W
1
2
3
1
2
3
36kD
22kD
16kD
Anti-αA
Anti-αB
Anti-β
Anti-γ
αB-C1
αB-C2
αB-C3
6kD
(B)
P0 Total Protein
P3 Total Protein
P7 Total Protein
P12 Total Protein
3W Total Protein
6W Total Protein
129
1
2
3
B6
Anti-αB
Actin
αB-C1
αB-C2
αB-C3

Figure 19. Western blotting of water insoluble proteins and total lens protein at different ages. (**A**) Western blotting of water insoluble proteins at 3W showed no significant differences in αA-, αB- and β-crystallin between D7Mit294 129/129 (*1*), 129/B6 (*2*), and B6/B6 (*3*), and there were less insoluble γ-crystallin in B6/B6 (*3*). At 6W, dramatic differences between the three genotypes are noted. There were more cleaved αA-, αB-, β- and γ-crystallins in severe 129/129 (*1*) and intermediate 129/B6 (*2*) than mild B6/B6 (*3*), indicated by arrowheads. This is most clearly represented in the cleavage of αB-crystallin (*αB-C1, αB-C2, αB-C3*). (**B**) Western blotting data of total lens proteins at P0, P3, P7, P12, 3W, and 6W of G0 129 α3 KO, D7Mit294 129/129 (*1*), 129/B6 (*2*), B6/B6 (*3*) and G0 B6 α3 KO. As indicated, there were more cleaved αB-crystallin cleavage in G0 129 α3 KO, D7Mit294 129/129, and D7Mit294 129/B6 than the D7Mit294 B6/B6 and G0 B6 α3 KO lenses, indicated by arrowheads.

4.4.5 Segregation of Other Genetic Modifier(s)

Since the G2 and F2 mice showed various phenotypes, we learned that there should be more than one suppressor in the B6 strain. Besides the one close to D7Mit294, we designed experiments to segregate other genetic modifier(s). As I mentioned above, the G3 mouse with very mild phenotype should contain most of the suppressors. Two mild phenotype G3 mice were intercrossed to generate F4 offspring. We genotyped all F4 mice and examined their lens opacities. We screened out mouse that showed mild phenotype but had two 129 alleles of the D7Mit294 locus. That particular mouse was backcrossed with 129 α3 knockout mice. Offspring showed different phenotypes at 6-week-old by examination. Lens pictures were captured (Figure 20), of note is that mice #2 and #3 displayed severe nuclear cataracts while mice #1, #4 and #5 showed intermediate phenotypes suggesting mice #1, #4 and #5 might contain the other genetic modifier(s) besides the one close to D7Mit294. Offspring from the same parents were examined at 6-week-old and mouse with mild to intermediate cataract phenotype was selected to backcross with 129 α3 knockout mouse. Another round of genetic linkage needs to be carried out in order to identify the other modifier(s).

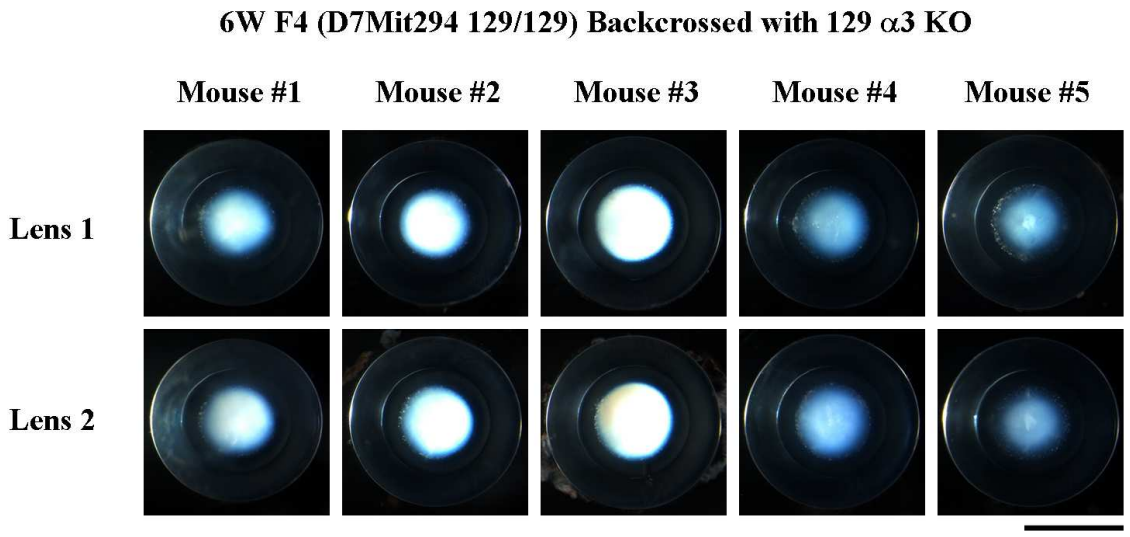

Figure 20. Lens pictures of offspring from F4 (D7Mit294 129/129) α3 knockout mouse backcrossed with 129 α3 knockout mouse. Five mice showed different phenotypes at 6-week-old: mice #2 and #3 displayed severe nuclear cataracts while mice #1, #4 and #5 showed intermediate phenotypes. Phenotypes of lens 1 and 2 are alike. Scale bar: 1mm.

4.4.6 One of the Genetic Suppressors Is Located Between D7Mit23 and D7Mit294.

We have identified a crossover mouse that came from intercross of two G13 mice, both of which had one B6 allele of D7Mit294 locus. Crossover founder mouse #1 was B6/B6 at D7Mit294 but B6/129 at D7Mit23. The founder was then backcrossed with 129 α3 knockout mice. Offspring were genotyped by D7Mit294 and D7Mit23 markers, and mice with one crossover B6 allele were selected (B6/129 at D7Mit294, 129/129 at D7Mit23). One of the female offspring was mated with founder male #1, different mouse genotypes were generated. Diagram of chromosomal composition was shown in Figure 21. Of note is that the lens picture of 7-month-old #1 mouse showed mild nuclear cataract with diffused powdery opacity throughout the lens. Mice #2 to #4 were same-age littermates that were from founder #1 crossing with its offspring. Mouse #2 containing one crossover allele and one longer allele of the B6 strain (indicated by one shorter and one longer green line) showed mildest lens phenotype. Mouse #3 with two crossover B6 alleles displayed mild nuclear cataract. However, mouse #4 with one regular long B6 allele and one 129 allele developed intermediate to severe type of nuclear cataract (Figure 21).

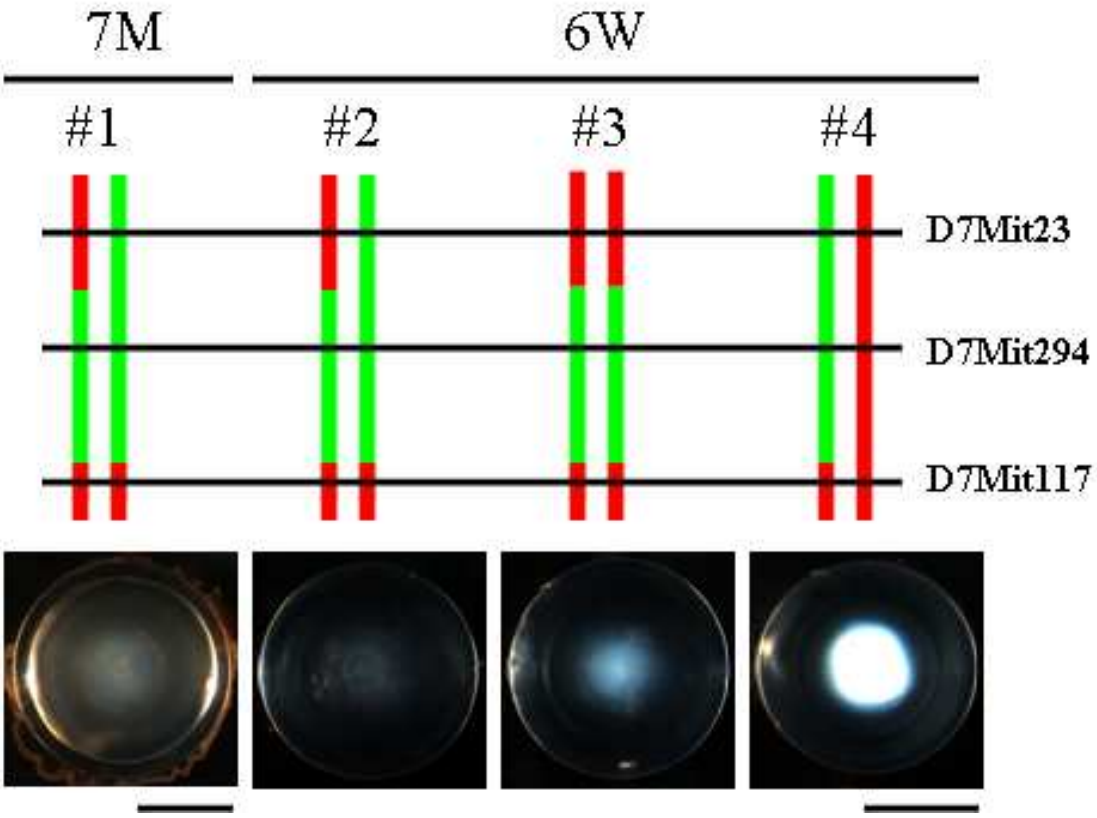

Figure 21. Lens pictures of crossover mice (7-month-old founder #1 and 6-week-old offspring #2 to #4). Founder #1 male mouse had a crossover allele of the B6 strain between D7Mit23 and D7Mit117 (indicated by shorter green line). The lens picture of #1 mouse at 7-month-old showed mild nuclear cataract with diffused powdery opacity throughout the lens (left image). Scale bar: 1mm. Mice #2 to #4 were from founder #1 crossing with its offspring that was generated by #1 backcrossing with 129 α3 knockout mice. Mouse #2 containing one crossover allele and one longer allele of the B6 strain (indicated by one shorter and one longer green line) showed mildest lens phenotype (second to the left). Mouse #3 with two crossover B6 alleles (indicated by two shorter green lines) displayed mild nuclear cataract (second to the right). However, littermate control #4 with one regular long B6 allele and one 129 allele developed intermediate to severe type of nuclear cataract (right image). Scale bar: 1mm.

4.5 Discussion

4.5.1 Summary

This work tries to map dominant genetic modifier(s) in C57BL/6J strain background that suppresses a severe nuclear cataract caused by α3 connnexin null mutation using classical genetic approaches. Multiple factors have been shown to play roles in influencing the severity of cataract. We have identified at least one suppressor which is located on the chromosome 7 of the B6 strain background near genetic marker D7Mit294. Two copies of B6 D7Mit294 alleles significantly reduce lens opacity in α3 knockout mice mostly in the 129 background. We have not conclusively narrowed down to a single gene or gene complex, fine mapping and candidate gene characterization will lead to the identification of this genetic modifier(s). We may be dealing with three types of scenarios: 1) Polymorphism in gene exon region between B6 and 129 strains that causes protein coding change; 2) Polymorphism in the promotor/gene regulatory region that causes gene expression and regulation change; 3) Polymorphism in the gene intron region that causes different gene splicing. Both cases 1 and 3 will lead to different protein formation which may perturb protein structure and function. Case 2 may affect protein activity and protein synthesis. Because of dramatic phenotypic difference between two strains, we speculate that protein coding change is likely to be the cause, but we still cannot rule out other possibilities.

Biochemical data indicate that the severity of nuclear cataracts is correlated with the amount of cleaved forms of crystallin proteins in α3 knockout lenses with different alleles of D7Mit294 of different strains. The modifier(s) near D7Mit294 behaves in a similar way like the original suppressors in the B6 strain which modulate crystallin protein degradation. However, the modifier(s) near D7Mit294 is not the only factor evidenced by 1) D7Mit294 B6/B6 lens phenotype is not as mild as the B6 α3 knockout lens; 2) the presence of 11-kD γ-crystallin in D7Mit294 B6/B6 lenses and αB-crystallin cleavages are more significant in D7Mit294 B6/B6 than B6 α3 knockout. Crystallin degradation is a consequence of an increase of calcium concentration and activation of Calpain proteases caused by a loss of gap junction communication formed by α3 connexin (Baruch et al., 2001; Gong et al., 1997). *In vitro* lens culture with and without specific calpain inhibitors implicates a lens calpain 3 isoform (Lp82/85) is associated with the formation of nuclear cataracts in α3 knockout mice (Baruch et al.). CAPN3 and α3 double knockout study clearly demonstrates that CAPN3 is required for the dense nuclear cataract formation in 129 α3 knockout mice (Tang 2008). However, double knockout mice in the 129 strain background still display a diffuse “powdery” cataract which is of different appearance with B6 α3 knockout lens. Because the CAPN3 gene is identical between 129 and B6 strains, it is unlikely that CAPN3 is the direct modifier, but that modification of calpain 3 activity may be accomplished via genetic suppressor(s).

4.5.2 Calpain Activity and Genetic Modifier

Previous work by our laboratory has shown that severity of nuclear cataract in 129 and B6 α3 knockout mice is correlated to the amount of cleaved αB- and γ-crystallin (Gong et al.). The initiation of the nuclear cataractogenesis can be correlated with the appearance of the cleaved form of αB-crystallin (Gong et al.), as we clearly observe αB-C2 cleavage at P0 in 129 α3 knockout and D7Mit294 129/129 samples. However, cleavage of αB-crystallin by itself is not sufficient for generation of a severe nuclear cataract because cleavages occur before dense opacity is observed. Rather, the cleavage of γ-crystallin may be more crucial for determine the severity of the nuclear cataract (Gong et al.), which is supported by the observation that D7Mit294 B6/B6 sample still has a little bit γ-crystallin cleavage while B6 α3 knockout has none, and D7Mit294 B6/B6 lens is slightly more opaque than B6 α3 knockout as stated above. Additional factor(s) is(are) needed to completely suppress the γ-crystallin cleavage, probably making the lens phenotype as mild as B6 α3 knockout. The cataract appearance in CAPN3 and α3 double knockout mice unlike a dense nuclear in α3 single knockout mice is probably due to the lack of smaller cleaved form of αB-crystallin (αB-C2) and 11-kD cleaved γ-crystallins (Tang et al), and Lp82/85 is suggested to lead to γ-crystallin cleavage in culture lenses (Baruch et al). Lp82/85 is responsible for these two protein cleavage forms. Presence of the 11-kD γ-crystallin cleavage band in D7Mit294 B6/B6 lens suggests Lp82/85 is still active but not as highly as in D7Mit294 129/129 lens. We have observed overall less crystallin cleavages in D7Mit294 B6/B6 lens not specifically αB-C2 and 11-kD γ-crystallins and it is shown before that m-calpain and μ-calpain can also cleave crystallin protein in a calcium dependent manner (David and Shearer, 1993; Robertson et al., 2008). This suggests that rather than only Lp82/85 activity, whole calpain activity seems to be reduced in mice with two B6 alleles of D7Mit294. One hypothesis is that the genetic suppressor near D7Mit294 inhibits the activation of the calpain proteases or their activities.

4.5.3 Calcium Homeostasis and Genetic Modifier

Calcium homeostasis is very important for maintaining lens transparency in humans and rodents (Duncan and Wormstone, 1999; Truscott et al., 1990). Mouse lenses are even more sensitive to calcium levels due to the presence of calcium-dependent proteases, such as calpains, especially the calpain 3 isoform (Lp82/Lp85) (Azuma et al., 1997; Nakamura et al., 2000; Tang et al., 2007). Elevated intracellular calcium levels activate calpains that cleave α- and β/γ-crystallin proteins (Tang et al., 2007; Ueda et al., 2002; Xia et al., 2006a). An alternative hypothesis is that the genetic modifier can regulate calcium homeostasis and/or inhibit calcium concentration rise so that calcium concentration never reaches a critical level to activate Lp82/85 and other calpains. Previous studies by Mathias' group have shown intracellular calcium concentration in 129 α3 knockout lens raises to around 2μM in the mature fibers compared to about 700nM range for wild-type lens, which is sufficient to activate Lp82/85 (critical level is about 1μM). The genetic modifier(s) near D7Mit294 may control the calcium increase in 129 α3 knockout lens so that Lp82/85 and other calpains are less active or inactive, thus, less crystallin degradation is observed. Intracellular calcium concentration measurement of B6 α3 knockout lens and D7Mit294 B6/B6 lens will lead us to understand calcium distribution in those lenses and consolidate this hypothesis.

4.5.4 Light Scattering Measurement and Quantification

Light scattering measurement and quantification allow us to precisely detect the subtle difference between cataractous lenses. It is done through a fiber optic spectrometer, unlike traditional grid grading system, objective factors are ruled out. Lenses are illuminated by a white light source perpendicular to the equator of the lens. Scattered light by any opacity is captured by the optic fiber with a whole acceptance of angle of 24.8°. The working angle sets a limitation to how much area it can measure, it may not be able to cover the whole mouse lens (depends on size of the lens), but it is able to cover at least the lens nucleus where nuclear cataract is located. So this technique is perfect for our application purpose to measure light scattering by nuclear cataractous lenses. With normalization to baseline each time taken, data is repeatable and comparable. The drawbacks of this technique is that light source intensity, distance between the light source and lens sample, daylight and fluorescent tube light bulb may influence the scattering results causing variations even sometime with the same sample. To minimize the light source effect, we use standardized fiber optic illuminator (Dolan-Jenner Industries, Inc) with low, medium and high level control of light intensity. High level light intensity is used and room light is turned off each time doing measurement. The distance between light source and lens sample can still vary, but we try our best to keep them around 1cm distances. We also snap at least two shots of light scattering measurement spectrum and average them for quantification purposes.

4.5.5 Recent Studies and Future Directions

A recent study of proteomic differences between 129 and B6 α3 knockout lenses provide useful information implicating some candidates for the genetic modifier (Hoehenwarter 2008). It is shown that HSP27/25 and ERp29 protein levels are upregulated in the B6 strain at a young age (Hoehenwarter 2008). However, there are no further studies or evidence suggesting these two proteins are genetic suppressors. Interestingly, their work also indicates that the 129 strain has about a 2-3 fold increase of low-molecular-weight αB-crystallin cleavage product in both wild-type and α3 knockout lenses (Hoehenwarter 2008). This may explain why αB-C2 is first clearly noticed at new born stage in mice without genetic suppressor, potentially associated with initiation of nuclear cataract.

In the previous subchapter 4.4.3, I have discussed that intercrossed mice with two 129 alleles of the D7Mit294 locus should show severe nuclear cataract in older generation intercrossed litters, given the possibility that we may have lost the other suppressors in the genome. However, in F4 mice, it is possible to see D7Mit294(129/129) mice display mild phenotypes because other suppressors played roles. We have filtered away the contribution by the modifier near D7Mit294 and successfully segregated the other suppressors in the B6 strain (subchapter 4.4.5). By using a similar genetic approach, we may identify other loci that are linked to the genetic modifier(s).

We are also fortunate to generate crossover mice that help us narrow down the genetic suppressor between D7Mit23 and D7Mit294 (subchapter 4.4.6). Mice with two crossover B6 alleles display milder phenotypes than mice with only one crossover or one regular B6 allele suggesting that the genetic modifier is located in between these two genetic markers. However, only from this one specific litter, the #3 mouse (two crossover B6 alleles) is a little bit more severe than the #2 mouse (one crossover and one regular B6 allele). This can be due to 1) the crossover allele may contain at least one suppressor, but there are other candidates that have been excluded; 2) individual mouse variation or sex variation. We have generally observed that male mice show less severe cataract phenotypes than female of the same genotype. The sex factor has not been elucidated. We need to investigate more litters to conclusively make the judgment.

Our next question is where the crossover allele ends between D7Mit23 and D7Mit294? Base on SNP (Single Nucleotide Polymorphism) in genes Cyp2b9 and Cy2a4 between B6 and 129 strains, we identify that the B6 alleles starts before Cyp2a4 gene (27.09M), but the end point has not been determined yet. Genotyping PCR suggests the end point is between D7Mit266 (29.09M) and D7Mit117 (30.71M).

In summary, studies of the genetic modifier on chromosome 7 of B6 strain near D7Mit294 marker suggest a novel genetic locus which contains genetic suppressor(s) for a nuclear cataract. This locus does not include those candidate genes reported by other groups, such as CAPN3, HSP27/25 and ERp29. Thus, the modifier in this locus will be a new candidate gene or gene complex. This work further supports that the suppressor on chromosome 7 behaves similarly as the original ones in B6 α3 knockout mice, sharing the mechanism where this modifier

specifically inhibits proteases and/or regulates calcium homeostasis to suppress severe nuclear cataracts. Discovery of this locus provides us with a unique opportunity to determine the altered signals that are caused by a decrease in gap junction communication formed by α3 connexins. We reveal that gap junction communication may be affected by extra factors. However, it is still unclear which gene/gene complex is the modifier. Further fine mapping and gene cloning will determine the possible candidates and identify a gene that has been so important in the gap junction field for the past decade.

Chapter 5 Gap Junction Communication and Cataracts

This thesis work indicates that regulation of gap junction communication in the lens affects lens transparency, revealing potential strategies for cataract prevention. We have shown that an increase in gap junction communication by knock-in α3 connexin can prevent a nuclear cataract caused by γB-crystallin-S11R mutation, while a decrease in gap junction communication by knockout α3 connexin promotes nuclear cataract, which is also influenced by genetic modifiers on Chr7 and another chromosome. . Further studies are needed to identify these genetic modifiers.

Investigation of a dominant nuclear cataractous mouse line *NM3062*, linked to the γB-crystallin S11R point mutation, revealed that abnormal γ-crystallin protein aggregation probably disrupted the membrane-cytoskeleton structures of fiber cells, which would lead calcium influx and calcium-dependent protein degradation. Degeneration of inner mature fiber cells and enlarged extracellular space cause a dense nuclear cataract.

Knock-in α3 connexin, replacing endogenous α8 connexin, increases the expression of α3 connexin and decrease calcium level in interior mature lens fiber cells. *Ki α3* mice provide us unique opportunity to test the hypothesis that increased gap junction communication may prevent nuclear cataract. *Ki α3* and *NM3062* compound mutant mice display clear lenses. Thus, prevention of interior fiber cell degeneration is probably dependent on the over-expression of α3 connexin, which enhances the intercellular communication and cell-cell adhesion to maintain normal calcium homeostasis and membrane-cytoskeleton structures in the lens. Previous studies show the deletion of the α3 connexin gene causes distinct nuclear cataracts in the 129/SvJ or C57BL/6J mouse strains. We successfully mapped one of the suppressors on chromosome 7 of C57BL/6J mouse strain. This suppressor is located in a region of ~3 million base pair near genetic marker D7Mit294. It remains not fully understood for how this genetic modifier influences the nuclear cataract, however, the cataract severity is associated with the amount of crystallin protein degradation. We hypothesize this genetic suppressor is likely inhibiting the activation of calpain proteases and/or regulating calcium homeostasis. In summary, this thesis demonstrates a fundamental concept that improved communication in the lens can prevent nuclear cataracts. Additional genetic factors play critical roles when communication is affected. Gap junction proteins and the genetic suppressor are good targets for anti-cataract agents.

References

Andley, U.P. (2007). Crystallins in the eye: Function and pathology. Prog Retin Eye Res *26*, 78-98.

Antuch, W., Guntert, P., and Wuthrich, K. (1996). Ancestral beta gamma-crystallin precursor structure in a yeast killer toxin. Nat Struct Biol *3*, 662-665.

Azuma, M., Fukiage, C., David, L.L., and Shearer, T.R. (1997). Activation of calpain in lens: a review and proposed mechanism. Exp Eye Res *64*, 529-538.

Baldo, G.J., Gong, X., Martinez-Wittinghan, F.J., Kumar, N.M., Gilula, N.B., and Mathias, R.T. (2001). Gap junctional coupling in lenses from alpha(8) connexin knockout mice. J Gen Physiol *118*, 447-456.

Baruch, A., Greenbaum, D., Levy, E.T., Nielsen, P.A., Gilula, N.B., Kumar, N.M., and Bogyo, M. (2001). Defining a link between gap junction communication, proteolysis, and cataract formation. J Biol Chem *276*, 28999-29006.

Bassnett, S. (2002). Lens organelle degradation. Exp Eye Res *74*, 1-6.

Bassnett, S., and Mataic, D. (1997). Chromatin degradation in differentiating fiber cells of the eye lens. J Cell Biol *137*, 37-49.

Beyer, E.C., Kistler, J., Paul, D.L., and Goodenough, D.A. (1989). Antisera directed against connexin43 peptides react with a 43-kD protein localized to gap junctions in myocardium and other tissues. J Cell Biol *108*, 595-605.

Bloemendal, H., de Jong, W., Jaenicke, R., Lubsen, N.H., Slingsby, C., and Tardieu, A. (2004). Ageing and vision: structure, stability and function of lens crystallins. Prog Biophys Mol Biol *86*, 407-485.

Brakenhoff, R.H., Aarts, H.J., Reek, F.H., Lubsen, N.H., and Schoenmakers, J.G. (1990). Human gamma-crystallin genes. A gene family on its way to extinction. J Mol Biol *216*, 519-532.

Candia, O.A. (2004). Electrolyte and fluid transport across corneal, conjunctival and lens epithelia. Exp Eye Res *78*, 527-535.

Chylack, L.T., Jr., Peterson, L.E., Feiveson, A.H., Wear, M.L., Manuel, F.K., Tung, W.H., Hardy, D.S., Marak, L.J., and Cucinotta, F.A. (2009). NASA study of cataract in astronauts (NASCA). Report 1: Cross-sectional study of the relationship of exposure to space radiation and risk of lens opacity. Radiat Res *172*, 10-20.

Clark, J.I., and Clark, J.M. (2000). Lens cytoplasmic phase separation. Int Rev Cytol *192*, 171-187.

Clout, N.J., Kretschmar, M., Jaenicke, R., and Slingsby, C. (2001). Crystal structure of the calcium-loaded spherulin 3a dimer sheds light on the evolution of the eye lens betagamma-crystallin domain fold. Structure *9*, 115-124.

Cotrina, M.L., Lin, J.H., and Nedergaard, M. (2008). Adhesive properties of connexin hemichannels. Glia *56*, 1791-1798.

Dahm, R., van Marle, J., Prescott, A.R., and Quinlan, R.A. (1999). Gap junctions containing alpha8-connexin (MP70) in the adult mammalian lens epithelium suggests a re-evaluation of its role in the lens. Exp Eye Res *69*, 45-56.
David, L.L., and Shearer, T.R. (1993). Beta-crystallins insolubilized by calpain II in vitro contain cleavage sites similar to beta-crystallins insolubilized during cataract. FEBS Lett *324*, 265-270.
De Maria, A.B., Shi, Y., Kumar, N.M., and Bassnett, S. (2009). Calpain expression and activity during lens fiber cell differentiation. J Biol Chem.
Delaye, M., and Tardieu, A. (1983). Short-range order of crystallin proteins accounts for eye lens transparency. Nature *302*, 415-417.
Derham, B.K., and Harding, J.J. (1999). Alpha-crystallin as a molecular chaperone. Prog Retin Eye Res *18*, 463-509.
Duncan, G., and Wormstone, I.M. (1999). Calcium cell signalling and cataract: role of the endoplasmic reticulum. Eye *13 (Pt 3b)*, 480-483.
Evans, P., Wyatt, K., Wistow, G.J., Bateman, O.A., Wallace, B.A., and Slingsby, C. (2004). The P23T cataract mutation causes loss of solubility of folded gammaD-crystallin. J Mol Biol *343*, 435-444.
Fischer, D., Hauk, T.G., Muller, A., and Thanos, S. (2008). Crystallins of the beta/gamma-superfamily mimic the effects of lens injury and promote axon regeneration. Mol Cell Neurosci *37*, 471-479.
Forrester, J., Dick, A., McMenamin, P., and Lee, W. (1996). The Eye: Basic Sciences in Practice (London: W.B. Saunders Company Ltd).
Frenzel, E.M., and Johnson, R.G. (1996). Gap junction formation between cultured embryonic lens cells is inhibited by antibody to N-cadherin. Dev Biol *179*, 1-16.
Fu, L., and Liang, J.J. (2002). Conformational change and destabilization of cataract gammaC-crystallin T5P mutant. FEBS Lett *513*, 213-216.
Gao, J., Sun, X., Martinez-Wittinghan, F.J., Gong, X., White, T.W., and Mathias, R.T. (2004). Connections between connexins, calcium, and cataracts in the lens. J Gen Physiol *124*, 289-300.
Giepmans, B.N. (2004). Gap junctions and connexin-interacting proteins. Cardiovasc Res *62*, 233-245.
Gong, X., Agopian, K., Kumar, N.M., and Gilula, N.B. (1999). Genetic factors influence cataract formation in alpha 3 connexin knockout mice. Dev Genet *24*, 27-32.
Gong, X., Baldo, G.J., Kumar, N.M., Gilula, N.B., and Mathias, R.T. (1998). Gap junctional coupling in lenses lacking alpha3 connexin. Proc Natl Acad Sci U S A *95*, 15303-15308.
Gong, X., Li, E., Klier, G., Huang, Q., Wu, Y., Lei, H., Kumar, N.M., Horwitz, J., and Gilula, N.B. (1997). Disruption of alpha3 connexin gene leads to proteolysis and cataractogenesis in mice. Cell *91*, 833-843.
Goodenough, D.A. (1992). The crystalline lens. A system networked by gap junctional intercellular communication. Semin Cell Biol *3*, 49-58.
Graw, J. (1997). The crystallins: genes, proteins and diseases. Biol Chem *378*, 1331-1348.

Graw, J. (2009). Genetics of crystallins: cataract and beyond. Exp Eye Res *88*, 173-189.
Graw, J., Coban, L., Liebstein, A., and Werner, T. (1991). Murine gamma E-crystallin is distinct from murine gamma 2-crystallin. Gene *104*, 265-270.
Graw, J., Liebstein, A., Pietrowski, D., Schmitt-John, T., and Werner, T. (1993). Genomic sequences of murine gamma B- and gamma C-crystallin-encoding genes: promoter analysis and complete evolutionary pattern of mouse, rat and human gamma-crystallins. Gene *136*, 145-156.
Greiner, J.V., and Chylack, L.T., Jr. (1979). Posterior subcapsular cataracts: histopathologic study of steroid-associated cataracts. Arch Ophthalmol *97*, 135-144.
Hejtmancik, J.F. (2008). Congenital cataracts and their molecular genetics. Semin Cell Dev Biol *19*, 134-149.
Hoehenwarter, W., Klose, J., and Jungblut, P.R. (2006). Eye lens proteomics. Amino Acids *30*, 369-389.
Hoehenwarter, W., Tang, Y., Ackermann, R., Pleissner, K.P., Schmid, M., Stein, R., Zimny-Arndt, U., Kumar, N.M., and Jungblut, P.R. (2008). Identification of proteins that modify cataract of mouse eye lens. Proteomics *8*, 5011-5024.
Horwitz, J. (1992). Alpha-crystallin can function as a molecular chaperone. Proc Natl Acad Sci U S A *89*, 10449-10453.
Horwitz, J. (2000). The function of alpha-crystallin in vision. Semin Cell Dev Biol *11*, 53-60.
Horwitz, J. (2003). Alpha-crystallin. Exp Eye Res *76*, 145-153.
Jobby, M.K., and Sharma, Y. (2007). Calcium-binding to lens betaB2- and betaA3-crystallins suggests that all beta-crystallins are calcium-binding proteins. Febs J *274*, 4135-4147.
John Forrester, A.D., Paul McMenamin, William Lee (1996). The Eye: Basic Sciences in Practice (London: W.B. Saunders Company Ltd).
Jongen, W.M., Fitzgerald, D.J., Asamoto, M., Piccoli, C., Slaga, T.J., Gros, D., Takeichi, M., and Yamasaki, H. (1991). Regulation of connexin 43-mediated gap junctional intercellular communication by Ca2+ in mouse epidermal cells is controlled by E-cadherin. J Cell Biol *114*, 545-555.
Kahn, H.A., Leibowitz, H.M., Ganley, J.P., Kini, M.M., Colton, T., Nickerson, R.S., and Dawber, T.R. (1977). The Framingham Eye Study. I. Outline and major prevalence findings. Am J Epidemiol *106*, 17-32.
Klein, B.E., Klein, R., Lee, K.E., and Grady, L.M. (2006). Statin use and incident nuclear cataract. JAMA *295*, 2752-2758.
Kurz, G.H., and Einaugler, R.B. (1968). Cataract secondary to microwave radiation. Am J Ophthalmol *66*, 866-869.
Li, L., Chang, B., Cheng, C., Chang, D., Hawes, N.L., Xia, C.H., and Gong, X. (2008). Dense nuclear cataract caused by the gammaB-crystallin S11R point mutation. Invest Ophthalmol Vis Sci *49*, 304-309.

Liu, H., Du, X., Wang, M., Huang, Q., Ding, L., McDonald, H.W., Yates, J.R., 3rd, Beutler, B., Horwitz, J., and Gong, X. (2005). Crystallin {gamma}B-I4F mutant protein binds to {alpha}-crystallin and affects lens transparency. J Biol Chem *280*, 25071-25078.
Lo, W.K. (1989). Visualization of crystallin droplets associated with cold cataract formation in young intact rat lens. Proc Natl Acad Sci U S A *86*, 9926-9930.
Lydahl, E. (1984). Infrared radiation and cataract. Acta Ophthalmol Suppl *166*, 1-63.
Mackay, D.S., Andley, U.P., and Shiels, A. (2004). A missense mutation in the gammaD crystallin gene (CRYGD) associated with autosomal dominant "coral-like" cataract linked to chromosome 2q. Mol Vis *10*, 155-162.
Martinez-Wittinghan, F.J., Sellitto, C., Li, L., Gong, X., Brink, P.R., Mathias, R.T., and White, T.W. (2003). Dominant cataracts result from incongruous mixing of wild-type lens connexins. J Cell Biol *161*, 969-978.
Martinez-Wittinghan, F.J., Sellitto, C., White, T.W., Mathias, R.T., Paul, D., and Goodenough, D.A. (2004). Lens gap junctional coupling is modulated by connexin identity and the locus of gene expression. Invest Ophthalmol Vis Sci *45*, 3629-3637.
Mathias, R.T., Rae, J.L., and Baldo, G.J. (1997). Physiological properties of the normal lens. Physiol Rev *77*, 21-50.
McAvoy, J.W., Chamberlain, C.G., de Iongh, R.U., Hales, A.M., and Lovicu, F.J. (1999). Lens development. Eye *13 (Pt 3b)*, 425-437.
Meyer, R.A., Laird, D.W., Revel, J.P., and Johnson, R.G. (1992). Inhibition of gap junction and adherens junction assembly by connexin and A-CAM antibodies. J Cell Biol *119*, 179-189.
Mills, I.A., Flaugh, S.L., Kosinski-Collins, M.S., and King, J.A. (2007). Folding and stability of the isolated Greek key domains of the long-lived human lens proteins gammaD-crystallin and gammaS-crystallin. Protein Sci *16*, 2427-2444.
Murer-Orlando, M., Paterson, R.C., Lok, S., Tsui, L.C., and Breitman, M.L. (1987). Differential regulation of gamma-crystallin genes during mouse lens development. Dev Biol *119*, 260-267.
Musil, L.S., and Goodenough, D.A. (1990). Gap junctional intercellular communication and the regulation of connexin expression and function. Curr Opin Cell Biol *2*, 875-880.
Nag, N., Peterson, K., Wyatt, K., Hess, S., Ray, S., Favor, J., Bogani, D., Lyon, M., and Wistow, G. (2007). Endogenous retroviral insertion in Cryge in the mouse No3 cataract mutant. Genomics *89*, 512-520.
Nakahara, M., Nagasaka, A., Koike, M., Uchida, K., Kawane, K., Uchiyama, Y., and Nagata, S. (2007). Degradation of nuclear DNA by DNase II-like acid DNase in cortical fiber cells of mouse eye lens. FEBS J *274*, 3055-3064.
Nakamura, Y., Fukiage, C., Shih, M., Ma, H., David, L.L., Azuma, M., and Shearer, T.R. (2000). Contribution of calpain Lp82-induced proteolysis to experimental cataractogenesis in mice. Invest Ophthalmol Vis Sci *41*, 1460-1466.
Nandrot, E., Slingsby, C., Basak, A., Cherif-Chefchaouni, M., Benazzouz, B., Hajaji, Y., Boutayeb, S., Gribouval, O., Arbogast, L., Berraho, A., *et al.* (2003). Gamma-D crystallin gene

(CRYGD) mutation causes autosomal dominant congenital cerulean cataracts. J Med Genet *40*, 262-267.
Neale, R.E., Purdie, J.L., Hirst, L.W., and Green, A.C. (2003). Sun exposure as a risk factor for nuclear cataract. Epidemiology *14*, 707-712.
Nishimoto, S., Kawane, K., Watanabe-Fukunaga, R., Fukuyama, H., Ohsawa, Y., Uchiyama, Y., Hashida, N., Ohguro, N., Tano, Y., Morimoto, T., *et al.* (2003). Nuclear cataract caused by a lack of DNA degradation in the mouse eye lens. Nature *424*, 1071-1074.
Norledge, B.V., Hay, R.E., Bateman, O.A., Slingsby, C., and Driessen, H.P. (1997). Towards a molecular understanding of phase separation in the lens: a comparison of the X-ray structures of two high Tc gamma-crystallins, gammaE and gammaF, with two low Tc gamma-crystallins, gammaB and gammaD. Exp Eye Res *65*, 609-630.
Oda, S., Watanabe, K., Fujisawa, H., and Kameyama, Y. (1980). Impaired development of lens fibers in genetic microphthalmia, eye lens obsolescence, Elo, of the mouse. Exp Eye Res *31*, 673-681.
Ohki, S.Y., Kariya, E., Hiraga, K., Wakamiya, A., Isobe, T., Oda, K., and Kainosho, M. (2001). NMR structure of Streptomyces killer toxin-like protein, SKLP: further evidence for the wide distribution of single-domain betagamma-crystallin superfamily proteins. J Mol Biol *305*, 109-120.
Pande, A., Annunziata, O., Asherie, N., Ogun, O., Benedek, G.B., and Pande, J. (2005). Decrease in protein solubility and cataract formation caused by the Pro23 to Thr mutation in human gamma D-crystallin. Biochemistry *44*, 2491-2500.
Pande, A., Pande, J., Asherie, N., Lomakin, A., Ogun, O., King, J., and Benedek, G.B. (2001). Crystal cataracts: human genetic cataract caused by protein crystallization. Proc Natl Acad Sci U S A *98*, 6116-6120.
Paul, D.L., Ebihara, L., Takemoto, L.J., Swenson, K.I., and Goodenough, D.A. (1991). Connexin46, a novel lens gap junction protein, induces voltage-gated currents in nonjunctional plasma membrane of Xenopus oocytes. J Cell Biol *115*, 1077-1089.
Piatigorsky, J. (1981). Lens differentiation in vertebrates. A review of cellular and molecular features. Differentiation *19*, 134-153.
Qu, C., Gardner, P., and Schrijver, I. (2009). The role of the cytoskeleton in the formation of gap junctions by Connexin 30. Exp Cell Res *315*, 1683-1692.
Quillen, D.A. (1999). Common causes of vision loss in elderly patients. Am Fam Physician *60*, 99-108.
Rafnsson, V., Olafsdottir, E., Hrafnkelsson, J., Sasaki, H., Arnarsson, A., and Jonasson, F. (2005). Cosmic radiation increases the risk of nuclear cataract in airline pilots: a population-based case-control study. Arch Ophthalmol *123*, 1102-1105.
Rajini, B., Graham, C., Wistow, G., and Sharma, Y. (2003). Stability, homodimerization, and calcium-binding properties of a single, variant betagamma-crystallin domain of the protein absent in melanoma 1 (AIM1). Biochemistry *42*, 4552-4559.

Rajini, B., Shridas, P., Sundari, C.S., Muralidhar, D., Chandani, S., Thomas, F., and Sharma, Y. (2001). Calcium binding properties of gamma-crystallin: calcium ion binds at the Greek key beta gamma-crystallin fold. J Biol Chem *276*, 38464-38471.

Robertson, L.J., David, L.L., Riviere, M.A., Wilmarth, P.A., Muir, M.S., and Morton, J.D. (2008). Susceptibility of ovine lens crystallins to proteolytic cleavage during formation of hereditary cataract. Invest Ophthalmol Vis Sci *49*, 1016-1022.

Rong, P., Wang, X., Niesman, I., Wu, Y., Benedetti, L.E., Dunia, I., Levy, E., and Gong, X. (2002). Disruption of Gja8 (alpha8 connexin) in mice leads to microphthalmia associated with retardation of lens growth and lens fiber maturation. Development *129*, 167-174.

Sanderson, J., Marcantonio, J.M., and Duncan, G. (2000). A human lens model of cortical cataract: Ca2+-induced protein loss, vimentin cleavage and opacification. Invest Ophthalmol Vis Sci *41*, 2255-2261.

Sandilands, A., Hutcheson, A.M., Long, H.A., Prescott, A.R., Vrensen, G., Loster, J., Klopp, N., Lutz, R.B., Graw, J., Masaki, S., *et al.* (2002). Altered aggregation properties of mutant gamma-crystallins cause inherited cataract. EMBO J *21*, 6005-6014.

Santhiya, S.T., Abd-alla, S.M., Loster, J., and Graw, J. (1995). Reduced levels of gamma-crystallin transcripts during embryonic development of murine Cat2nop mutant lenses. Graefes Arch Clin Exp Ophthalmol *233*, 795-800.

Sellitto, C., Li, L., and White, T.W. (2004). Connexin50 is essential for normal postnatal lens cell proliferation. Invest Ophthalmol Vis Sci *45*, 3196-3202.

Sharma, Y., Rao, C.M., Narasu, M.L., Rao, S.C., Somasundaram, T., Gopalakrishna, A., and Balasubramanian, D. (1989). Calcium ion binding to delta- and to beta-crystallins. The presence of the "EF-hand" motif in delta-crystallin that aids in calcium ion binding. J Biol Chem *264*, 12794-12799.

Shentu, X., Yao, K., Xu, W., Zheng, S., Hu, S., and Gong, X. (2004). Special fasciculiform cataract caused by a mutation in the gammaD-crystallin gene. Mol Vis *10*, 233-239.

Shimeld, S.M., Purkiss, A.G., Dirks, R.P., Bateman, O.A., Slingsby, C., and Lubsen, N.H. (2005). Urochordate betagamma-crystallin and the evolutionary origin of the vertebrate eye lens. Curr Biol *15*, 1684-1689.

Siezen, R.J., Fisch, M.R., Slingsby, C., and Benedek, G.B. (1985). Opacification of gamma-crystallin solutions from calf lens in relation to cold cataract formation. Proc Natl Acad Sci U S A *82*, 1701-1705.

Slingsby, C., and Clout, N.J. (1999). Structure of the crystallins. Eye *13 (Pt 3b)*, 395-402.

Spencer, R.W., and Andelman, S.Y. (1965). Steroid Cataracts. Posterior Subcapsular Cataract Formation in Rheumatoid Arthritis Patients on Long Term Steroid Therapy. Arch Ophthalmol *74*, 38-41.

Sperduto, R.D., and Seigel, D. (1980). Senile lens and senile macular changes in a population-based sample. Am J Ophthalmol *90*, 86-91.

Talla, V., Srinivasan, N., and Balasubramanian, D. (2008). Visualization of in situ intracellular aggregation of two cataract-associated human gamma-crystallin mutants: lose a tail, lose transparency. Invest Ophthalmol Vis Sci *49*, 3483-3490.

Tang, Y., Liu, X., Zoltoski, R.K., Novak, L.A., Herrera, R.A., Richard, I., Kuszak, J.R., and Kumar, N.M. (2007). Age-related cataracts in alpha3Cx46-knockout mice are dependent on a calpain 3 isoform. Invest Ophthalmol Vis Sci *48*, 2685-2694.

Truscott, R.J., Marcantonio, J.M., Tomlinson, J., and Duncan, G. (1990). Calcium-induced opacification and proteolysis in the intact rat lens. Invest Ophthalmol Vis Sci *31*, 2405-2411.

Ueda, Y., Duncan, M.K., and David, L.L. (2002). Lens proteomics: the accumulation of crystallin modifications in the mouse lens with age. Invest Ophthalmol Vis Sci *43*, 205-215.

Wang, K., Cheng, C., Li, L., Liu, H., Huang, Q., Xia, C.H., Yao, K., Sun, P., Horwitz, J., and Gong, X. (2007a). {gamma}D-Crystallin Associated Protein Aggregation and Lens Fiber Cell Denucleation. Invest Ophthalmol Vis Sci *48*, 3719-3728.

Wang, K., Cheng, C., Li, L., Liu, H., Huang, Q., Xia, C.H., Yao, K., Sun, P., Horwitz, J., and Gong, X. (2007b). GammaD-crystallin associated protein aggregation and lens fiber cell denucleation. Invest Ophthalmol Vis Sci *48*, 3719-3728.

Wei, C.J., Francis, R., Xu, X., and Lo, C.W. (2005). Connexin43 associated with an N-cadherin-containing multiprotein complex is required for gap junction formation in NIH3T3 cells. J Biol Chem *280*, 19925-19936.

Wenk, M., Baumgartner, R., Holak, T.A., Huber, R., Jaenicke, R., and Mayr, E.M. (1999). The domains of protein S from Myxococcus xanthus: structure, stability and interactions. J Mol Biol *286*, 1533-1545.

White, T.W. (2002). Unique and redundant connexin contributions to lens development. Science *295*, 319-320.

White, T.W., Bruzzone, R., Goodenough, D.A., and Paul, D.L. (1992). Mouse Cx50, a functional member of the connexin family of gap junction proteins, is the lens fiber protein MP70. Mol Biol Cell *3*, 711-720.

White, T.W., Gao, Y., Li, L., Sellitto, C., and Srinivas, M. (2007). Optimal lens epithelial cell proliferation is dependent on the connexin isoform providing gap junctional coupling. Invest Ophthalmol Vis Sci *48*, 5630-5637.

White, T.W., Goodenough, D.A., and Paul, D.L. (1998). Targeted ablation of connexin50 in mice results in microphthalmia and zonular pulverulent cataracts. J Cell Biol *143*, 815-825.

Wistow, G., Wyatt, K., David, L., Gao, C., Bateman, O., Bernstein, S., Tomarev, S., Segovia, L., Slingsby, C., and Vihtelic, T. (2005). gammaN-crystallin and the evolution of the betagamma-crystallin superfamily in vertebrates. Febs J *272*, 2276-2291.

Xia, C.H., Cheng, C., Huang, Q., Cheung, D., Li, L., Dunia, I., Benedetti, L.E., Horwitz, J., and Gong, X. (2006a). Absence of alpha3 (Cx46) and alpha8 (Cx50) connexins leads to cataracts by affecting lens inner fiber cells. Exp Eye Res *83*, 688-696.

Xia, C.H., Cheung, D., DeRosa, A.M., Chang, B., Lo, W.K., White, T.W., and Gong, X. (2006b). Knock-in of alpha3 connexin prevents severe cataracts caused by an alpha8 point mutation. J Cell Sci *119*, 2138-2144.